1 **The Influence of Carbon Cycling on Oxygen Depletion in North-Temperate Lakes**

3 Austin Delany[1], Robert Ladwig[1], Cal Buelo[1], Ellen Albright[1], Paul C. Hanson[1]

4 [1] Center for Limnology, University of Wisconsin-Madison, Madison, WI, USA

5 *Correspondence to*: Austin Delany (addelany@wisc.edu)

7 **Abstract.** Hypolimnetic oxygen depletion during summer stratification in lakes can lead to

8 hypoxic and anoxic conditions. Hypolimnetic anoxia is a water quality issue with many

9 consequences, including reduced habitat for cold-water fish species, reduced quality of

10 drinking water, and increased nutrient and organic carbon (OC) release from sediments. Both

11 allochthonous and autochthonous OC loads contribute to oxygen depletion by providing

12 substrate for microbial respiration; however, their relative importance in depleting oxygen

13 across diverse lake systems remains uncertain. Lake characteristics, such as trophic state,

14 hydrology, and morphometry are also influential in carbon cycling processes and may impact

15 oxygen depletion dynamics. To investigate the effects of carbon cycling on hypolimnetic

16 oxygen depletion, we used a two-layer process-based lake model to simulate daily

17 metabolism dynamics for six Wisconsin lakes over twenty years (1995-2014). Physical

18 processes and internal metabolic processes were included in the model and were used to

19 predict dissolved oxygen (DO), particulate OC (POC), and dissolved OC (DOC). In our

20 study of oligotrophic, mesotrophic, and eutrophic lakes, we found autochthony to be far more

21 important than allochthony to hypolimnetic oxygen depletion. Autochthonous POC

22 respiration in the water column contributed the most towards hypolimnetic oxygen depletion

23 in the eutrophic study lakes. POC water column respiration and sediment respiration had

24 similar contributions in the mesotrophic and oligotrophic study lakes. ~~Differences in source~~

25 ~~of respiration are discussed with consideration of lake productivity.~~ Differences in source of

26 respiration are discussed with consideration of lake productivity and the processing and fates

27 of organic carbon loads.

29
30
31
32
33
34
35
36
37
38
39
40
41
42
43
44
45
46
47
48
49
50
51
52
53
54
55
56
57
58
59
60
61
62
63
64
65

1 Introduction

Hypolimnetic oxygen depletion impacts lake ecosystems through its influences on lake habitat and organic carbon (OC) cycling (Cole & Weihe 2016). In many lakes, oxygen depletion results in hypoxia and even anoxia (Nürnberg 1995). Hypolimnetic anoxia reduces habitat availability for cold-water fish species (Magee et al. 2019), reduces quality of drinking water (Bryant et al. 2011), and can lead to elevated nutrient and OC release from lake sediments (Hoffman et al. 2013, McClure et al. 2020). The formation of hypolimnetic anoxia is associated with many internal and external lake characteristics, such as trophic status (Rhodes et al., 2017; Rippey & McSorley, 2009), lake morphometry (Livingstone & Imboden, 1996), and hydrology (Nürnberg 2004). An increase in the prevalence of hypolimnetic anoxia and associated water quality degradation in temperate lakes indicates the need to better understand how lake ecological processes interact with external forcing to lead to the development of anoxia (Jane et al. 2021).

Hypolimnetic anoxia can occur when water column and sediment microbial respiration rates exceed rates of oxygenation over an extended period. The conditions supporting oxygen depletion are the outcomes of complex ecosystem processes and the interactions of the lake with its climate and landscape settings (Jenny et al. 2016a, 2016b). Autochthonous OC inputs vary considerably across trophic gradients and are a labile substrate for microbial respiration that can contribute substantially to hypolimnetic anoxia (Müller et al. 2012, 2019). Allochthonous OC sources have also been shown to impact dissolved oxygen (DO)

90   and carbon dynamics in lakes by providing a more consistent and recalcitrant substrate for

91   respiration (Hanson et al. 2014, Solomon et al. 2015). Non-biological factors can be

92   important as well, such as the watershed loading of allochthonous OC, which can influence

93   the overall lability of OC in a lake and the rate of DO depletion (Hotchkiss et al. 2018).

94   Physical factors, such as stratification onset, water column stability, and vertical mixing, can

95   control the transport of DO from oxygen-rich upper layers to the lower layers of a lake, and

96   can therefore limit oxygen availability in the hypolimnion (Snortheim et al. 2017, Ladwig et

97   al. 2021). Lake morphometry can influence the spatial extents of stratified layers, which can

98   have profound effects on hypolimnetic volume and its capacity to hold DO as well as the rate

99   of sediment oxygen consumption, which can both influence anoxia onset in lakes

100 (Livingstone & Imboden 1996). Thus, the sources and lability of OC, lake morphometry, and

101 lake hydrodynamics all contribute to hypolimnetic oxygen depletion rates, making it an

102 emergent ecosystem property with a plethora of causal relationships to other ecologically

103 important variables.

104

105 Although previous studies have investigated contributions of allochthonous and

106 autochthonous OC to lake carbon cycling (Hanson et al. 2014, McCullough et al. 2018), the

107 effects on formation of hypolimnetic anoxia deserves further exploration (Hanson et al.

108 2015). The magnitude and relative balance of the sources of OC loads relates to hypolimnetic

109 anoxia across trophic and hydrology gradients (Rhodes et al., 2017; Rippey and McSorley,

110 2009, Hanson et al. 2014). These gradients affect the relative contributions of autochthony

111 and allochthony in a lake, which further control the lability and fates (respiration, burial,

export) of OC. The lability of OC relates to its form and its source (Hotchkiss et al. 2018, Catalán et al. 2016). Autochthonous POC and DOC tend to be much more labile than allochthonous OC (Amon & Brenner 1996, Thorpe & Delong 2002), thus understanding both the forms of OC and their origins, in addition to their magnitudes, informs our understanding of the controls over lake respiration. Quantifying the contribution of these different factors to hypolimnetic anoxia is crucial to understanding its drivers across lakes and through time.

The availability of long-term observational data combined with process-based models provides an opportunity to investigate OC sources and their control over the dynamics of lake DO across multiple time scales. Long-term studies of lakes on regional and global scales highlight how environmental trends can influence metabolic processes in lakes, and how lakes can broaden our understanding of large-scale ecosystem processes (Richardson et al. 2017, Kraemer et al. 2017, Williamson et al. 2008). For example, long-term studies allow us to investigate the impact that current and legacy conditions have on lake ecosystem function in a given year (Carpenter et al. 2007). Process-based modeling has been used to investigate metabolism dynamics and understand both lake carbon cycling (Hanson et al. 2004, Cardille et al. 2007) and formation of anoxia (Ladwig et al. 2022); however, explicitly tying lake carbon cycling and metabolism dynamics with long-term hypolimnetic DO depletion across a variety of lakes remains largely unexplored. The combination of process-based modeling with available long-term observational data, including exogenous driving data representative of climate variability, can be especially powerful for recreating representations of long-term lake metabolism dynamics (Staehr et al. 2010, Cardille et al. 2007).

134

135 ~~In this study, our goal is to investigate OC source contributions to lake carbon cycling and~~

136 ~~hypolimnetic oxygen depletion. We are particularly interested in the relative loads of~~

137 ~~autochthonous and allochthonous OC to lakes and how they contribute to hypolimnetic DO~~

138 ~~depletion across seasonal to decadal scales. We use a process-based lake metabolism model,~~

139 ~~combined with daily external driving data and long-term limnological data, to study six lakes~~

140 ~~within the North Temperate Lakes Long-Term Ecological Research network (NTL LTER)~~

141 ~~over a twenty-year period (1995-2014). We address the following questions: (1) What are the~~

142 ~~dominant sources of organic carbon that contribute to hypolimnetic oxygen depletion, and~~

143 ~~how do their contributions differ across a group of diverse lakes over two decades? (2) How~~

144 ~~do lake trophic state, hydrology, and morphometry influence the processing and fates of~~

145 ~~organic carbon loads in ways that affect hypolimnetic dissolved oxygen?~~

146 Hypolimnetic oxygen depletion is a persistent and global phenomenon that degrades lake

147 ecosystems services (Nurnberg 1995; Cole & Weihe 2016; Jenny et al. 2016). In lakes where

148 oxygen depletion results in hypoxia and even anoxia, habitat availability for cold-water fish

149 species is eliminated (Magee et al. 2019), quality of drinking water is reduced (Bryant et al.

150 2011), and nutrient and OC release from lake sediments becomes elevated (Hoffman et al.

151 2013, McClure et al. 2020). An increase in the prevalence of hypolimnetic anoxia and

152 associated water quality degradation in temperate lakes indicates the need to better

153 understand how lake ecological processes interact with external forcings, such as hydrology

154 and nutrient inputs, to control the development of anoxia (Jenny et al, 2016 a,b).

155

Allochthonous organic carbon (OC) loading to lakes that explains the prevalence of negative net ecosystem production (i.e., net heterotrophy) provides substrate for hypolimnetic oxygen depletion (Houser et al. 2003). Allochthonous OC sources have also been shown to influence dissolved oxygen (DO) and carbon dynamics in lakes by providing recalcitrant substrate for respiration (Cole et al. 2002; Hanson et al. 2014, Solomon et al. 2015). In lake surveys, dissolved allochthonous OC correlates positively with net heterotrophy ((Jansson et al. 2000), indicating the importance of allochthony to both the carbon balance and dynamics of dissolved gases (Prairie et al. 2002; Hanson et al. 2003). However, the persistent and often stable concentration of allochthonous DOC in the water column of lakes also indicates its recalcitrant nature, raising the question of whether allochthony alone can support high oxygen demand in the sediments and deeper waters of lakes.

The contributions of OC from autochthony to hypolimnetic oxygen depletion may be important as well, despite its low concentrations relative to that of allochthonous OC in many lakes (Cole et al. 2002). Autochthonous OC tends to be highly labile (Amon & Brenner 1996, Thorpe & Delong 2002), and spot samples from lake surveys may not detect autochthonous DOC, reducing its power as a correlate of ecosystem function. Positive correlation between anoxia and lake phosphorus concentrations suggests autochthony may contribute substantially to hypolimnetic oxygen demand (Rhodes et al. 2017; Rippey & McSorley, 2009; Jenny et al. 2016a,b); however, the link between nutrient concentrations, autochthony, and hypolimnetic respiration is rarely quantified. Lakes with high autochthony can still be net heterotrophic (Staehr et al. 2010; Cole et al. 2000), however, it matters where in the lake autochthony is respired. Export of phytoplankton from the epilimnion to the hypolimnion and

sediments contributes to deep water oxygen demand (Müller et al. 2012; Rhodes et al. 2017; Beutel 2003), and the magnitude and timing of organic carbon inputs to deeper waters in lakes and the subsequent fate of that carbon deserves further exploration.

Understanding the relative importance of autochthony and allochthony to hypolimnetic oxygen depletion requires consideration of a number of physical and biological processes controlling oxygen sources and sinks in lakes (Hanson et al. 2015). For dimictic north temperate lakes, the timing and dynamics of seasonal stratification determine the ambient temperature and light conditions for metabolism and the extent to which the hypolimnion is isolated from oxygen-rich surface waters (Snortheim et al. 2017, Ladwig et al. 2021). In many lakes, the hypolimnion is below the euphotic zone, but in very clear lakes, primary production within the hypolimnion may be an oxygen source (Houser et al. 2003). Lake morphometry influences the spatial extents of stratified layers, which determines the ratio of hypolimnetic volume to sediment surface area and the magnitude the sediment oxygen sink for the hypolimnetic oxygen budget (Livingstone & Imboden 1996). Thus, the sources and labilities of OC, lake morphometry, and lake hydrodynamics all contribute to hypolimnetic oxygen budgets, making it an emergent ecosystem property with a plethora of causal relationships to other ecologically important variables.

The availability of long-term observational data combined with process-based models provides an opportunity to investigate OC sources and their control over the dynamics of lake DO across multiple time scales. Long-term studies of lakes on regional and global scales highlight how environmental trends can influence metabolic processes in lakes, and how

lakes can broaden our understanding of large-scale ecosystem processes (Richardson et al.

2017, Kraemer et al. 2017, Williamson et al. 2008). For example, long-term studies allow us

to investigate the impact that current and legacy conditions have on lake ecosystem function

in a given year (Carpenter et al. 2007). Process-based modeling has been used to investigate

metabolism dynamics and understand both lake carbon cycling (Hanson et al. 2004, Cardille

et al. 2007) and formation of anoxia (Ladwig et al. 2022); however, explicitly tying lake

carbon cycling and metabolism dynamics with long-term hypolimnetic DO depletion across a

variety of lakes remains largely unexplored. The combination of process-based modeling

with available long-term observational data, including exogenous driving data representative

of climate variability, can be especially powerful for recreating representations of long-term

lake metabolism dynamics (Staehr et al. 2010, Cardille et al. 2007).

In this study, our goal is to investigate OC source contributions to lake carbon cycling and

hypolimnetic oxygen depletion. We are particularly interested in the relative loads of

autochthonous and allochthonous OC to lakes and how they contribute to hypolimnetic DO

depletion across seasonal to decadal scales. We use a process-based lake metabolism model,

combined with daily external driving data and long-term limnological data, to study six lakes

within the North Temperate Lakes Long-Term Ecological Research network (NTL LTER)

over a twenty-year period (1995-2014). We address the following questions: (1) What are the

dominant sources of organic carbon that contribute to hypolimnetic oxygen depletion, and

how do their contributions differ across a group of diverse lakes over two decades? (2) How

does lake trophic state influence the processing and fates of organic carbon loads in ways that

affect hypolimnetic dissolved oxygen?

225

2 Methods

2.1 Study Site

This study includes six Wisconsin lakes from the NTL-LTER program (Magnuson et al.

2006). Trout Lake (TR), Big Muskellunge Lake (BM), Sparkling Lake (SP), and Allequash

Lake (AL) are in the Northern Highlands Lake District of Wisconsin and have been regularly

sampled since 1981 (Magnuson et al. 2006). Lake Mendota (ME) and Lake Monona (MO)

are in southern Wisconsin and have been regularly sampled by the NTL-LTER since 1995

(NTL-LTER, Magnuson et al. 2006). The NTL-LTER provides a detailed description of each

lake (Magnuson et al. 2006). The six lakes span gradients in size, morphometry, landscape

setting, and hydrology, which creates diverse carbon cycling characteristics and processes

across these systems. TR and AL are drainage lakes with high allochthonous carbon inputs

from surface water, while BM and SP are groundwater seepage systems with allochthony

dominated by aerial OC inputs from the surrounding landscape (Hanson et al. 2014). All four

northern lakes (TR, AL, BM, SP) are surrounded by a forested landscape. ME and MO are

both eutrophic drainage lakes surrounded by an urban and agricultural landscape. Although

the full range of DOC concentrations for lakes in northern Wisconsin varies from about 2 to

>30 mg L^{-1} (Hanson et al. 2007), DOC concentrations among our study lakes covered a

relatively narrow range typical of non-dystrophic lakes in Wisconsin (Hanson et al. 2007)

and are near the global averages previously estimated, i.e., 3.88 mg/L (Toming et al. 2020)

and 5.71 mg/L (Sobek et al. 2007), respectively. Morphometry, hydrology, and other

information can be found in Table 1.

247

Table 1. Physical and biogeochemical characteristics of the study lakes. The table includes lake area (Area), maximum depth (Zmax), hydrologic residence time (RT), mean annual temperature (Temp), mean annual surface total phosphorus concentration (Mean TP), and mean annual surface DOC (Mean DOC).

252

Lake	Area (ha)	Zmax (m)	RT [3,4] (years)	Temp [2] (°C)	Mean TP [1] (µgL)	Mean DOC [1] (mgL)
Allequash Lake (AL)	168.4	8	0.73	10.5	14	3.9
Big Muskellunge (BM)	396.3	21.3	5.1	10.5	7	3.8
Sparkling Lake (SP)	64	20	8.88	10.6	5	3.12
Trout Lake (TR)	1607.9	35.7	5.28	9.8	5	2.8
Mendota (ME)	3961	25.3	4.3	12.5	50	5.6
Monona (MO)	1324	22.5	0.7	13.8	47	5.8

253

1 - Magnuson et al. (2020, 2006)
2 - Magnuson et al. (2022)
3 - Hunt et al. (2013)
4 - Webster et al. (1996)

258

259

260

261 **2.2 Driving Data and Limnological Data**

262   Most driving data for the model is provided by the "Process-based predictions of water

263   temperature in the Midwest US" USGS data product (Read et al. 2021). This includes lake

264   characteristic information such as lake area and hypsometry, daily modeled temperature

265   profiles, ice flags, meteorology data, and solar radiation for the six study lakes. Derived

266   hydrology data is used in calculating daily OC loading and outflow for the study lakes.

267   Hydrology for the northern lakes is taken from Hunt & Walker (2017), which was estimated

268   using a surface and groundwater hydrodynamic model. Hydrology for ME is taken from

269   Hanson et al. (2020), which used the Penn State Integrated Hydrologic Model (Qu & Duffy

270   2007). We assume for ME and MO that evaporation from the lake surface is approximately

271   equal to precipitation on the lake surface and that groundwater inputs and outputs to the lake

272   are a small part of the hydrologic budgets (Lathrop & Carpenter 2014). Therefore, ME

273   outflow is assumed to be equal to ME inflow. ME is the predominant hydrologic source for

274   MO (Lathrop & Carpenter 2014), thus, MO inflow is assumed to be equal to ME outflow,

275   and MO outflow is assumed to be equal to MO inflow. We found that the derived discharge

276   data for ME, TR, AL, and SP was approximately 20-50% higher than previously reported

277   values (Hunt et al. 2013, Webster et al. 1996), depending on the lake, while hydrology in BM

278   was approximately 25% too low (Hunt et al. 2013). To accommodate this issue, we adjusted

279   total annual hydrological inputs to match published water residence times for each lake

280   (Table 1), while retaining temporal hydrological patterns. NTL-LTER observational data are

281   interpolated to estimate daily nutrient concentration values, which are used in calculating

282   daily primary production in the model (Magnuson et al. 2020).

283

284   The NTL-LTER observational data used to calibrate and validate the model for the six lakes

285   include DO, DOC, and Secchi depth (Magnuson et al. 2020, Magnuson et al. 2022).

286   Saturation values for DO and gas exchange velocity used in calculating atmospheric

287   exchange for DO are calculated using the "o2.at.sat.base" and using the Cole and Caraco gas

288   exchange method from the "K600.2.KGAS.base" function within the USGS

289   "LakeMetabolizer" package in R (Winslow et al. 2016).

290

291   **2.3 The Model**

292   The goal of our model is to use important physical and metabolic processes involved in the

293   lake ecosystem carbon cycle to best predict DO, DOC, and POC, while keeping the model

294   design simple in comparison with more comprehensive water quality models (e.g., Hipsey et

295   al. 2019 2022). We ran our model with a daily time step over a twenty-year period (1995-

296   2014) for each lake and included seasonal physical dynamics, such as lake mixing,

297   stratification, and ice cover from Read et al. 2021. Throughout each year, the model tracks

298   state variables and fluxes in the lake for each day (Fig. 1). These state variables include DO

299   and the labile and recalcitrant components of particulate organic carbon (POC) and dissolved

300   organic carbon (DOC). Initial conditions for each state variable are based on literature

301   values or lake observational data (SI Table 5). The model is initialized on January 1st of the

302   first year, so we set the initial labile POC mass to zero under the assumption that the

303   concentration is low in the middle of winter. The initial DO value is set to the saturation

304   value based on the conditions of the initial model run day and is calculated using the

305   LakeMetabolizer R package (Winslow et al. 2016). During stratified periods, the state

306   variables and fluxes for the epilimnion and hypolimnion are tracked independently.

307   Atmosphere, sediments, and hydrologic inputs and outputs are boundary conditions.

308
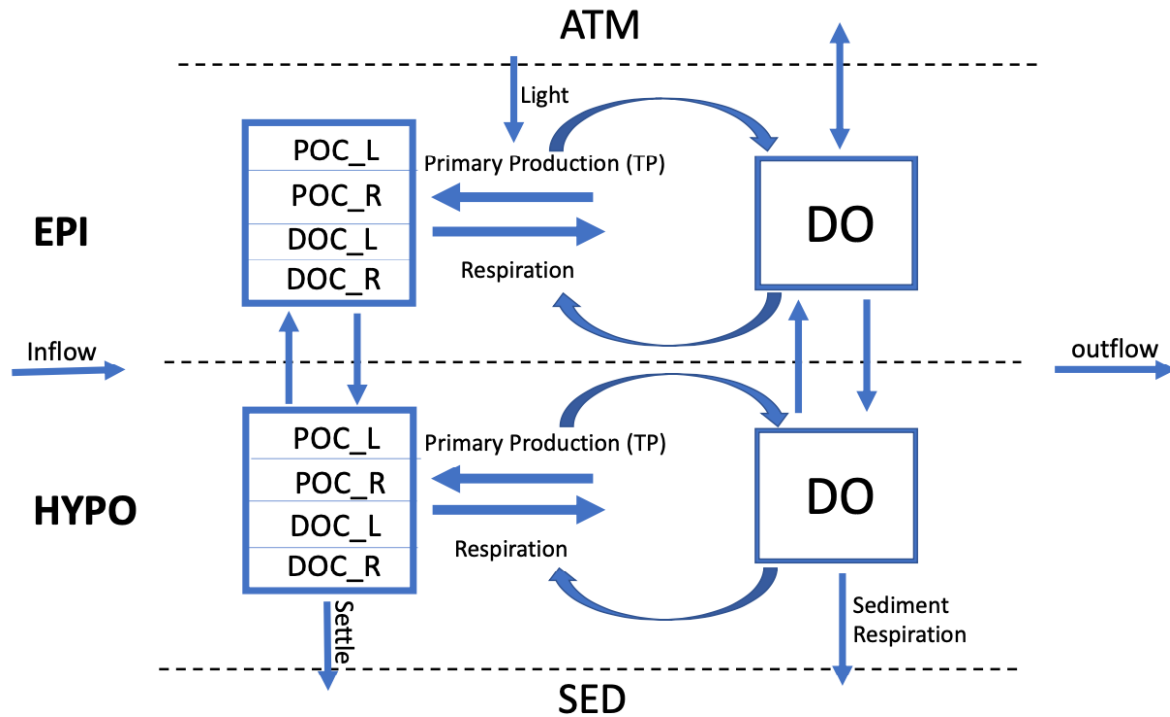
309
310   **Figure 1.** Conceptual lake model showing state variables (boxes) and fluxes (arrows). The
311   model has two thermal layers under stratified conditions, as shown here, and tracks state
312   variables separately for each layer. The sediment (SED), atmosphere (ATM), inflow and
313   outflow are system boundaries. The state variables included are DO (dissolved oxygen),
314   DOC_L (labile dissolved organic carbon), DOC_R (recalcitrant dissolved organic carbon),
315   POC_L (labile particulate organic carbon), and POC_R (recalcitrant particulate organic
316   carbon). ~~Inorganic carbon (IC) is not tracked in the model and is assumed to be a non-~~
317   ~~limiting substrate to primary production.~~ Observed total phosphorus (TP) is used as a driving
318   variable for primary production in the model.
319

320   The model is built specifically for this analysis; however, many of the assumptions around

321   the model complexity and mathematical formulations are borrowed from literature cited

322   (Ladwig et al. 2022, Hipsey et al. 2022, Hanson et al. 2014, McCullough et al. 2018). We

323   chose to develop our own process-based model rather than use an existing model, such as

324   GLM (Hipsey et al. 2022) or Simstrat (Goudsmit et al. 2002), so that we could simulate and

325   measure the specific metabolism fluxes related to our study questions.

326

2.3.1 Stratification Dynamics

328   Lake physical dynamics are taken from the output of a previous hydrodynamic modeling

329   study on these same lakes over a similar time period (Read et al. 2021), which used the

330   General Lake Model (Hipsey et al. 2019). Before running the metabolism model, a

331   thermocline depth for each time step is estimated using derived temperature profiles for each

332   lake (Read et al. 2021) by determining the center of buoyancy depth (Read et al. 2011). After

333   calculating the thermocline depth, the volumes and average temperatures for each layer, and

334   the specific area at thermocline depth are determined using lake-specific hypsography. The

335   criteria for stratification include a vertical density gradient between the surface and bottom

336   layer of at least 0.05 kg m^{-3}, an average water column temperature above 4 °C, and the

337   presence of a derived thermocline (Ladwig et al. 2022). For any day that does not meet all of

338   these criteria, the water column is considered to be fully mixed. The thermocline depth

339   values are smoothed using a moving average with a window size of 14 days to prevent large

340   entrainment fluxes that can destabilize the model at very short time scales when thermal

341   strata are shallow. During mixed periods, the entire lake is treated as the epilimnion, and a

342   separate hypolimnion is not incorporated into the model dynamics. Ice cover in the model is

343   determined using the "ice flag" provided in the derived temperature profile data from Read et

344   al. (2021). Our metabolism model does simulate under-ice conditions, however we do not

345   include the presence of inverse stratification during winter periods.

346

2.3.2 External Lake and Environment Physical Fluxes

Atmospheric exchange of DO, external loading of OC, and outflow of OC are the three

environmental boundary fluxes accounted for in the water quality model (Table 3 Eq. 9-11).

The gas exchange velocity for atmospheric exchange is determined using the Cole and

Caraco model (1998) and is calculated using the LakeMetabolizer R package (Winslow et al.

2016). Oxygen saturation values are also calculated using this package. During ice covered

conditions, we assume that the atmospheric exchange value is ten percent of the value during

non-ice covered conditions based on sea ice gas exchange estimates (Loose and Schlosser,

2011).

356

For the northern lakes (TR, AL, BM, SP), we use the allochthonous OC load and recalcitrant

OC export values from Hanson et al. (2014) to calibrate total annual allochthonous OC load

and recalcitrant OC export in our model. We specifically use the allochthonous OC load

values in this study to assist in the manual calibration of inflow recalcitrant POC and DOC

concentrations for each lake. For the southern lakes (ME, MO), we also use derived

hydrology information (Hanson et al. 2020), but only for discharge that is the inflow for ME.

We assume for ME and MO that evaporation from the lake surface is approximately equal to

precipitation on the lake surface and that groundwater inputs and outputs to the lake are a

small part of the hydrologic budgets (Lathrop & Carpenter 2014). Therefore, ME outflow is

assumed to be equal to ME inflow. ME is the predominant hydrologic source for MO

(Lathrop & Carpenter 2014), thus, MO inflow is assumed to be equal to ME outflow, and

368 ~~MO outflow is assumed to be equal to MO inflow. ME allochthonous load is calibrated based~~

369 ~~on model fitting and observational data (Hart et al. 2019). MO inflow concentrations are~~

370 ~~equivalent to the in-lake epilimnetic concentrations of OC from ME at each model time step.~~

371 ~~The OC loads for MO are calibrated based on the total allochthonous load found in~~

372 ~~McCullough et al. 2018.~~

373

374 For the northern lakes (TR, AL, BM, SP), we assume that allochthonous OC loads consist of

375 entirely recalcitrant substrates. We verify total OC load, total inflow concentration, and

376 recalcitrant OC export values with estimates from Hanson et al. (2014). For ME, we verify

377 the total annual allochthonous OC load and OC inflow concentrations against observed

378 inflow data from Hart et al. (2017) by back calculating inflow concentrations based on the

379 modeled OC equilibrium of the lake. MO inflow concentrations are equivalent to the in-lake

380 epilimnetic concentrations of OC from ME at each model time step. The total OC loads for

381 MO are verified based on the total allochthonous load found in McCullough et al. 2018.

382

383 **Table 2.** Equations for the model, organized by state variables, [DO (dissolved oxygen),
384 $DOCL$ (labile dissolved organic carbon), $DOCR$(recalcitrant dissolved organic carbon),
385 $POCL$ (labile particulate organic carbon), $POCR$ (recalcitrant particulate organic carbon),
386 $Secchi$] and relevant fluxes. *Note:* The entrainment flux ($Entr$) is only included during
387 thermally stratified periods. The inflow (IN) and outflow (OUT) fluxes are not included in
388 the calculations for the hypolimnetic layer. The inflow of labile DOC (IN_{DOCL}) parameter in
389 Eq. 2 is only used for calculating allochthonous OC loads for MO. Atmospheric gas
390 exchange of dissolved oxygen ($AtmExch$) is not included for the hypolimnetic DO
391 calculation. Normalized total phosphorus is represented by (TP_{norm}). The volume (V) term
392 represents the respective lake layer volume, or the discharge volume for the inflow and
393 outflow equations. The term (r_{rate}) is included in Eq. 13 to represent the respiration rates of
394 the different OC pools. It is included to simplify the table of equations. Terms not defined
395 here are included in Table 3.
396

State Variables

DO [gDO] $\frac{dDO}{dt} = (NPP * O2_{convert}) + AtmExch + Entr_{DO} - (R_{sed} * O2_{convert}) - (R_{wc} * O2_{convert})$	(1)
DOCL [gC] $\frac{dDOC_L}{dt} = (NPP * (1 - C_{NPP})) + IN_{DOCL} + Entr_{DOCL} - R_{DOCL} - OUT_{DOCL}$	(2)
DOCR [gC] $\frac{dDOC_R}{dt} = IN_{DOCR} + Entr_{DOCR} - OUT_{DOCR} - R_{DOCR\ Epi}$	(3)
POCL [gC] **Mixed and Epi:** $\frac{dPOC_L}{dt} = (NPP_{Epi} * C_{NPP}) + IN_{POCL} + Entr_{POCL} - R_{POCL\ Epi} - Settle_{POCL\ Epi} - OUT_{POCL}$ **Hypo:** $\frac{dPOC_L}{dt} = (NPP_{Hypo} * C_{NPP}) + Settle_{POCL\ Epi} - Settle_{POCL\ Hypo} - R_{POCL\ Hypo} - Ent_{POCL}$	(4) (5)
POCR [gC] **Mixed and Epi:** $\frac{dPOC_R}{dt} = IN_{POCR} + Entr_{POCR} - OUT_{POCR} - R_{POCR\ Epi} - Settle_{POCR\ Epi}$ **Hypo:** $\frac{dPOC_R}{dt} = Settle_{POCR\ Epi} - Settle_{POCR\ Hypo} - R_{POCR\ Hypo} - Entr_{POCR}$	(6) (7)
Secchi [m] $Secchi = \frac{1.7}{K_{LEC}}$	(8)
Fluxes	
Atm exchange [gDO d^{-1}] $AtmExch = K_{DO} * (DO_{sat} - DO_{prediction}) * Area_{sfc}$	(9)
Inflow [gC d^{-1}] $IN = Carbon\ Concentration_{inflow} * V_{inflow}$	(10)
Outflow [gC d^{-1}] $OUT = Carbon\ Concentration_{outflow} * V_{outflow}$	(11)
Net Primary Productivity [gC d^{-1}] $NPP = Pmax * (1 - e^{(-IP*\frac{Light}{Pmax})}) * TP_{norm} * \theta_{NPP}^{(T-20)} * V$	(12)
Respiration [gC d^{-1}] $R_{wc} = Carbon\ Pool * r_{rate} * \theta_{Resp}^{(T-20)} * \frac{DO\ Concentration}{DO_{1/2} + DO\ Concentration}$	(13)
Sediment Respiration [gC d^{-1}] $R_{sed} = r_{sed} * \theta_{Resp}^{(T-20)} * \frac{DO\ Concentration}{DO_{1/2} + DO\ Concentration} * Area_{sed}$	(14)
POC settle [gC d^{-1}] $Settle = (POC\ Pool * K_{POC}) * \frac{Area}{V}$	(15)
Entrainment [gC d^{-1}] $V_{Entr} = V_{epi}(t) - V_{epi}(t-1)$ $\quad V_{Entr} > 0$ (Epilimnion growing) $\quad\quad Entr = \frac{V_{Entr}}{V_{Hypo}} * Carbon\ Pool_{Hypo}$ $\quad V_{Entr} < 0$ (Epilimnion shrinking) $\quad\quad Entr = \frac{V_{Entr}}{V_{Epi}} * Carbon\ Pool_{Epi}$	(16) (17) (18)
Light [W m^{-2}] $Light = \int_{z_1}^{z_2}(I_{z_1} * e^{-(K_{LEC} * z)})\,dz * (1 - \alpha)$	(19)
Light Extinction Coefficient [Unitless] $K_{LEC} = LEC_{water} + (LEC_{POC} * ((\frac{POCL}{V}) + (\frac{POCR}{V}))) + (LEC_{DOC} * ((\frac{DOCL}{V}) + (\frac{DOCR}{V})))$	(20)

397

2.3.3 Internal Lake Physical Fluxes

The two in-lake physical fluxes included in the model are POC settling and entrainment of all

state variables. POC settling is the product of a sinking rate (m d^{-1}) and the respective POC

pool (g), divided by the layer depth (m) (Table 3 Eq. 15). Sinking rates are either borrowed

from literature values (Table 3) or fit during model calibration (see below). Entrainment is

calculated as a proportion of epilimnetic volume change (Table 2 Eq. 17-18). A decrease in

epilimnetic volume shifts mass of state variables from the epilimnion into the hypolimnion,

and an increase in volume shifts mass from the hypolimnion to the epilimnion.

Table 3. Model Parameters, grouped into three categories: constants, which are values that were not tuned; manually calibrated, which are parameters manually tuned, typically guided by ranges from the literature; and parameters calibrated through constrained parameter search, which are calibrated through an automated search of parameter space.

Parameter	Abbreviation	Value	Units	Source
Constants				
Conversion of Carbon to Oxygen	$O2_{convert}$	2.67	Unitless	Mass Ratio of C:O
Respiration rate of DOCR	r_{DOCR}	0.001	day^{-1}	(Hanson et al., 2011)
Respiration rate of POCR	r_{POCR}	0.005	day^{-1}	Taken from ranges provided in (Hanson et al. 2004)
Respiration rate of POCR	r_{POCR}	0.005	day^{-1}	Taken from ranges provided in (Hanson et al. 2004)
Respiration rate of POCL	r_{POCL}	0.2	day^{-1}	Taken from ranges provided in (Hipsey et al. 2022)

Parameter	Abbreviation	Value	Units	Source
Michaelis-Menten DO half saturation coefficient	$DO_{1/2}$	0.5	$g\ m^{-3}$	Taken from ranges provided in (Hipsey et al. 2022)
Light extinction coefficent of water	LEC_{water}	0.125	m^{-1}	Taken from ranges in Hart et al. (2017)
Ratio of DOC to POC production from NPP	C_{NPP}	0.8	Unitless	Biddanda & Benner (1997)
Albedo	α	0.3	Unitless	Global average (Marshall & Plumb, 2008)
Atmospheric gas exchange adjustment during ice covered conditions	C_{winter}	0.1	Unitless	Taken from ranges in (Loose & Schlosser, 2011)
Coefficient of light transmitted through ice	C_{ice}	0.05	Unitless	Taken from ranges provided in (Lei et al. 2011)
Settling velocity rate of POC_R	K_{POCR}	1.2	$m\ day^{-1}$	Taken from ranges found in (Reynolds et al.1987)
Settling velocity rate of POC_L	K_{POCL}	1	$m\ day^{-1}$	Taken from ranges ranges found in (Reynolds et al.1987)
Temperature scaling coefficient for NPP	θ_{NPP}	1.12	Unitless	Taken from values provided in (Hipsey et al. 2022) and (Ladwig et al. 2022)
Temperature scaling coefficient for Respiration	θ_{Resp}	1.04	Unitless	Taken from values provided in (Hipsey et al. 2022) and (Ladwig et al. 2022)
Manually calibrated				
Light extinction of DOC	LEC_{DOC}	0.02 - 0.06	$m^2 g^{-1}$	Manually calibrated based on observed Secchi Depth ranges for the study lakes

Parameter	Abbreviation	Value	Units	Source
Light extinction of POC	LEC_{POC}	0.7	$m^2 g^{-1}$	Manually calibrated based on observed Secchi Depth ranges for the study lakes
Maximum Daily Productivity	$Pmax$	0.5-5	$g\ m^{-3} day^{-1}$	Manually calibrated from mean productivity values from Wetzel (2001)
Recalcitrant DOC inflow concentration	$DOCR_{inflow}$	5-10	$g\ m^{-3}$	Based on ranges found in (Hanson et al. 2014, McCullough et al. 2018, Hart et al. 2017)
Recalcitrant POC inflow concentration	$POCR_{inflow}$	2-5	$g\ m^{-3}$	Based on ranges found in (Hanson et al. 2014, McCullough et al. 2018, Hart et al. 2017)
Calibrated through constrained parameter search				
Slope of the irradiance/productivity curve	IP	0.045, 0.015	$gCd^{-1}(Wm^{-2})^{-1}$	Based on ranges found in (Platt et al. 1980) and tuned separately for each lake region (South, North)
Sediment respiration flux	r_{SED}	0.05 – 0.4	$g\ m^{-2} day^{-1}$	Based on ranges found in (Ladwig et al. 2021) and (Mi et al. 2020) and fit independently for each lake
Respiration rate of DOCL	r_{DOCL}	0.015 - 0.025	day^{-1}	Based on ranges found in (McCullough et al. 2018) and fit for each lake independently

415

416

2.3.4 Internal Lake Metabolism Fluxes

The metabolism fluxes in the model are net primary production (NPP) and respiration (R).

Respiration includes water column respiration for each OC state variable in the epilimnion

and hypolimnion and is calculated at each time step as the product of the OC state variable

421   and its associated first order decay rate (Table 2, Eq. 13). Sediment respiration for the

422   hypolimnion during stratified periods and the epilimnion (entire lake) during mixed periods

423   is a constant daily rate that is individually fit for each lake. Note that we did not include

424   anaerobic carbon metabolism in our modeling approach and discuss potential shortcomings

425   in the discussion section. We assume inorganic carbon is not a limiting carbon source. In the

426   model, we consider any DO concentration less than 1 g DO m^{-3} to be anoxic (Nürnberg

427   1995).

428

429   NPP is tracked in both the epilimnion and hypolimnion. NPP is a function of light, total

430   phosphorus concentration, temperature, a maximum productivity coefficient, and a slope

431   parameter defining the irradiance and productivity curve (Table 2 Eq. 12). We compared our

432   coefficients for primary production with those found in (Wetzel, 2001), which are in the

433   following units [mgC/m2/day]. Note that such coefficients are not per unit phosphorus, but

434   rather, subsume lake-specific nutrient concentrations. In order to do our comparison, we

435   subsumed nutrient concentrations into our calculations of primary production. Our approach

436   was to remove the mean of observed P and normalize by the P variance. Those two statistical

437   features of P become subsumed in the estimates of IP and Pmax, but the time dynamics of

438   normalized P are retained to represent seasonal P dynamics in the lake. Average light in a

439   layer is calculated for each day and is dependent on the depth of a layer and the light

440   extinction coefficient (Table 2 Eq. 19). During ice covered conditions, average light is

441   assumed to be five percent of the average non-ice covered value (Lei et al. 2011). Total

442   phosphorus concentration in a layer is from observational data for each lake interpolated to

443 ~~the daily time scale. The interpolated values are then normalized for each individual lake to~~

444 ~~drive NPP. These values are normalized so that differences among lakes are only present in~~

445 ~~the IP and P_{max} parameters. The Arrhenius equation provides temperature control for NPP,~~

446 ~~and we determined through model fitting a Θ of 1.12. OC derived from NPP is split between~~

447 ~~particulate and dissolved labile OC production, with eighty percent produced as POC and~~

448 ~~twenty percent produced as DOC. This ratio was determined through model fitting and is~~

449 ~~similar to previously reported values (Hipsey et al. 2019).~~

450 NPP is tracked in both the epilimnion and hypolimnion. NPP is a function of light, total

451 phosphorus concentration, temperature, a maximum productivity coefficient (*Pmax*), and a

452 slope parameter defining the irradiance and productivity curve (*IP*) (Table 2 Eq. 12). Total

453 phosphorus concentration in a layer taken is from observational data for each lake

454 interpolated to the daily time scale. Maximum daily primary production rates were taken

455 from Wetzel (2001). As these maximum production rates are not phosphorus-specific but

456 subsume lake-specific nutrient concentrations, we multiplied them with time-transient,

457 normalized TP concentrations. Normalizing was done by removing the mean of observed TP

458 and dividing by TP variance. This allows us to retain the time dynamics of the normalized

459 TP, which we use to represent seasonal TP dynamics for each lake. The Arrhenius equation

460 provides temperature control for NPP, and we determined through model fitting a Θ of 1.12.

461 All OC derived from NPP is assumed to be labile and is split between particulate and

462 dissolved OC production, with eighty percent produced as POC and twenty percent produced

463 as DOC. This ratio was determined through model fitting and is similar to previously

464 reported values (Hipsey et al. 2022). Average light in a layer is calculated for each day and is

465 dependent on the depth of a layer and the light extinction coefficient (Table 2 Eq. 19). During

466 ice covered conditions, average light is assumed to be five percent of the average non-ice

467 covered value (Lei et al. 2011).

468

469 Epilimnetic and hypolimnetic water column respiration is tracked independently for each OC

470 pool in the model. During mixed periods, there are four OC pools – DOCR, DOCL, POCR,

471 POCL. During stratified periods, those pools are split into a total of eight pools that are

472 tracked independently for the epilimnion and hypolimnion. Respiration is calculated as a

473 product of the mass of a respective variable, a first order decay rate coefficient, temperature,

474 and oxygen availability (Table 2 Eq. 13). The respiration decay rate coefficients are based on

475 literature values (Table 3) or were fit during model calibration. An Arrhenius equation is

476 used for temperature control of respiration, with θ_{Resp} equal to 1.04, which was determined

477 through manual model fitting. The respiration ~~rates~~ fluxes are also scaled by oxygen

478 availability using the Michaelis-Menten equation with a half saturation coefficient of 0.5 g

479 DO m^{-3}, such that at very low DO concentrations, the respiration flux approaches zero.

480

481 Sediment respiration is calculated from a constant daily respiration flux, adjusted for

482 temperature and oxygen availability, using the Arrhenius and Michaelis-Menten equations,

483 respectively (Table 2 Eq. 14). The mass of sediment OC is not tracked in the model. During

484 stratified periods, we assume that the majority of epilimnetic sediment area is in the photic

485 zone, and therefore has associated productivity from macrophytes and other biomass. It is

486 assumed that this background productivity and sediment respiration are of similar magnitude

487   and inseparable from water column metabolism, given the observational data. Therefore,

488   epilimnetic sediment respiration is not accounted for in the model during stratified

489   conditions. During mixed conditions, we assume that sediment respiration is active on all

490   lake sediment surfaces, which are assumed to be equivalent in area to the total surface lake

491   area. During stratified periods, we use the area at the thermocline as the sediment area for

492   calculating hypolimnetic sediment respiration.

493

494   **2.3.5 Other in-lake calculations and assumptions**

495   We calculate a total light extinction coefficient (LEC) for the epilimnion and hypolimnion.

496   The total LEC for each layer is calculated by multiplying the dissolved and particulate

497   specific LEC values with their respective OC state variable concentrations, combined with a

498   general LEC value for water (Table 2 Eq. 20). This total LEC value is used to calculate a

499   daily estimate of Secchi depth (Table 2 Eq. 8). The coefficients for the light extinction of

500   water, DOC, and POC are manually calibrated based on observed Secchi depth ranges for the

501   study lakes (Table 3, SI Table 5).

502

503   ~~2.4 Model calibration and validation~~

504   ~~The model was run for twenty years from 1 January 1995 to 31 December 2014. This period~~

505   ~~was chosen due to an absence of hydrologic data for the northern lakes after 2014 and~~

506   ~~because consistent observational data weren't available for the southern lakes until 1995. The~~

507   ~~first 15 years of the model output was used for calibration and the last 5 years were used for~~

508   ~~model validation. We chose the first 15 years for calibration because the observational data~~

509 were relatively stable and were not indicative of any large trends in ecosystem processes, as

510 opposed to the last five years which showed slightly more model deviation from DOC

511 observational data in the southern lakes (SI Fig. 2).

512

513 Initial conditions for each lake state variable are based on literature values or lake

514 observational data (SI Table 5). The model is initialized on January 1st of the first year, so

515 we set the initial labile POC mass to zero under the assumption that the concentration is low

516 in the middle of winter. The initial DO value is set to the saturation value based on the

517 conditions of the initial model run day and is calculated using the LakeMetabolizer R

518 package (Winslow et al. 2016).

519

520 **2.5 Model Fitting and Parameter Uncertainty Estimation**

521 The free parameters in the model are the slope of the irradiance/productivity curve (IP), the

522 respiration rate of labile DOC (Resp_DOCL), and the respiration rate of the hypolimnetic

523 sediments (Resp_sed) (Table 3). These were in part chosen due to the high uncertainty

524 around the parameter values, and our assumptions that they have a higher impact on

525 ecosystem dynamics in the model. Optimized values and uncertainties for each free

526 parameter and lake are included in SI Table 4.

527

528 IP controls the amount of productivity in low light scenarios, and fitting the parameter helps

529 to calibrate productivity during ice-covered winter conditions as well as during times of high

530 OC concentrations in the epilimnion. Resp_DOCL controls the seasonal dynamics of DOC in

a lake and treating it as a free parameter helps capture the across-lake variability in DOC processes related to variations in landscape, hydrology, and productivity. Resp_sed is important for controlling hypolimnetic oxygen depletion in lakes and is related to lake productivity and associated legacy OC in each lake. The Resp_sed parameter also helps adjust burial rates for the study lakes. We fit unique IP and Resp_DOCL values for the southern lake region (ME, MO), and unique values for the northern region (TR, AL, BM, SP). Resp_sed is individually fit for each lake.

We manually optimized free parameters by manually adjusting them over their respective ranges to find the parameter values that returned the smallest model residuals (SI Table 4). Automated optimization proved too computationally demanding. To gain a better sense of the contributions of parameter uncertainty in the model, we created parameter uncertainty distributions using standard deviations of 20% of the estimated parameter value. To evaluate the influence of parameter uncertainties on model predictions, the parameter distributions are randomly sampled over 100 model iterations to create the uncertainty bounds for all predictions of model state variables and fluxes.

During the model fitting, errors in modeled DO, DOC, and Secchi depth are weighted equally in the southern lakes. In the northern lakes, fitting Secchi depth was challenging. Initial model fits revealed that patterns in observed Secchi did not show regular seasonality and were highly stochastic. Therefore, we use a moving average on observational data and predictions of Secchi depth and calculate the residuals as the difference between the two

553 averaged time series. This is done to remove stochasticity from the observational data and fit

554 the model predictions to the average observed Secchi value. We use a moving average

555 window of 15 observations because we want to capture the average annual Secchi depth

556 trend, and there are roughly 15 observations per year.

557 **2.4 Model Sensitivity and Parameter Calibration**

558 To better understand the sensitivities of the model output to parameter values, we performed

559 a sensitivity analysis of the model parameters using the global sensitivity method from

560 Morris (1991). The sensitivity analysis showed that there were nine parameters to which the

561 model was consistently sensitive across the six study lakes. This group included the ratio of

562 DOC to POC produced from NPP (C_{NPP}), the maximum daily productivity parameter

563 (*Pmax*), the inflow concentration of recalcitrant POC ($POCR_{inflow}$), the setting velocity of

564 recalcitrant POC (K_{POCR}), the temperature fitting coefficients for productivity and respiration

565 (θ_{NPP}, θ_{Resp}) the slope of the irradiance/productivity curve (*IP*), the sediment respiration flux

566 (r_{SED}), and the respiration rate of DOCL (r_{DOCL}). We chose a subset of the nine parameters to

567 include in the uncertainty analysis based on the following justifications. The model results

568 showed that recalcitrant substrates are of lesser importance for lake metabolism dynamics, so

569 we chose not to further investigate the uncertainty of the $POCR_{inflow}$ and K_{POCR} parameters.

570 The *Pmax* and *IP* parameters are directly correlated, so we chose to remove Pmax from

571 further uncertainty considerations. The θ_{NPP} and θ_{RESP} parameters act as substitutes for water

572 temperature, a well-known "master variable" in water quality modeling, and directly reflect

573 seasonality in the model. Therefore, we chose to omit these parameters for further

574 uncertainty calculations. The final subset of parameters for uncertainty analysis consisted of

575   C_{NPP}, r_{DOCL}, r_{SED}, and *IP*. Of the four parameters, we felt C_{NPP} was best constrained by the

576   literature. To reduce the number of parameters estimated in the calibration process we

577   restricted the automated constrained parameter search to the remaining three.

578
579   Model parameters are grouped into three categories: constants, manually calibrated, and

580   parameters calibrated through an automated constrained parameter search. The constant

581   parameters are consistent across the study lakes and are not tuned. The manually calibrated

582   parameters were allowed to vary by lake and are typically guided by ranges from the

583   literature. The constrained parameter search uses an automated search of parameter space,

584   constrained by literature values, to fit the *IP*, r_{SED}, and r_{DOCL} parameters for the study lakes.

585   Specifically, we performed a constrained fitting of the model to observational data using the

586   Levenberg-Marquardt algorithm within the "modFit" function of the "FME" R package

587   (Soetaert & Petzoldt, 2010).

588
589   The first 15 years of the model output was used for calibration and the last 5 years were used

590   for model validation. We chose the first 15 years for calibration because the observational

591   data were relatively stable and were not indicative of any large trends in ecosystem

592   processes, as opposed to the last five years which showed slightly more model deviation

593   from DOC observational data in the southern lakes (SI Fig. 2).

594

595   **2.5 Model Uncertainty**

596   Sensitivity guided the uncertainty analysis. To quantify uncertainty around model

597   predictions, we sampled *IP*, r_{SED}, and r_{DOCL} simultaneously from uniform distributions

598   defined by +-30% of the literature ranges used for our calibrated parameter values (Table 3).

599   We ran one hundred model iterations randomly sampling the three model state variables

600   across these distributions. We plotted the minimum and maximum values for these uniform

601   distributions and included them in the time series plots (Fig. 2, 3, 4, SI Fig. 1,2,3).

602

603   **3 Results**

604
605   **3.1 Model Fit to Ecosystem States**

606   Model predictions of DO reproduce observed seasonal variability well. Note that RMSE

607   values presented here represent model error combined over both the validation and

608   calibration periods (see Supplementary Material: Table S1 for calibration and validation

609   specific RMSE values), and that state variables are presented with truncated time ranges for

610   visual clarity (see Supplementary Material: Fig. S1-S3 for full time series). Epilimnetic DO

611   generally has lower RMSE than DO in the hypolimnion (Fig. 2). ~~In the epilimnion, RMSE~~

612   ~~ranges from 0.73 g DO m^{-3} (TR) to 2.11 g DO m^{-3} (ME), and in the hypolimnion, RMSE~~

613   ~~ranges from 1.20 g DO m^{-3} (TR) to 2.69 g DO m^{-3} (AL).~~ In the epilimnion, RMSE ranges

614   from 0.74 g DO m^{-3} (TR) to 2.11 g DO m^{-3} (MO), and in the hypolimnion, RMSE ranges from

615   1.22 g DO m^{-3} (ME) to 2.77 g DO m^{-3} (AL, SP). Validation NSE values for DO ranged from -

616   1.45 (AL) to 0.02 (ME) in the epilimnion and -0.30 (SP) to 0.86 (ME) in the hypolimnion.

617   Validation KGE values for DO ranged from 0.40 (AL) to 0.90 (TR) in the epilimnion and

618   0.35 (SP) to 0.80 (ME) in the hypolimnion. KGE and NSE values for all lakes can be found

619   in SI Table 7. In the southern lakes, modeled values reach anoxic levels and generally follow

620   the DO patterns recorded in the observed data (Fig. 2a-b). Observational data for the northern

621 lakes show an occasional late summer onset of anoxia, and these events are generally

622 captured in the model output. A late summer spike in hypolimnetic DO predictions

623 commonly occurs as well, which is likely a model artifact caused by the reduction of

624 hypolimnetic volumes to very small values over short time periods prior to fall mixing.

625 Reduction to small volumes, coincident with modest fluxes due to high concentration

626 gradients, result in transient high concentrations. Overall, the goodness-of-fit of hypolimnetic

627 DO in our study lakes does not seem to follow any regional or lake characteristic patterns.
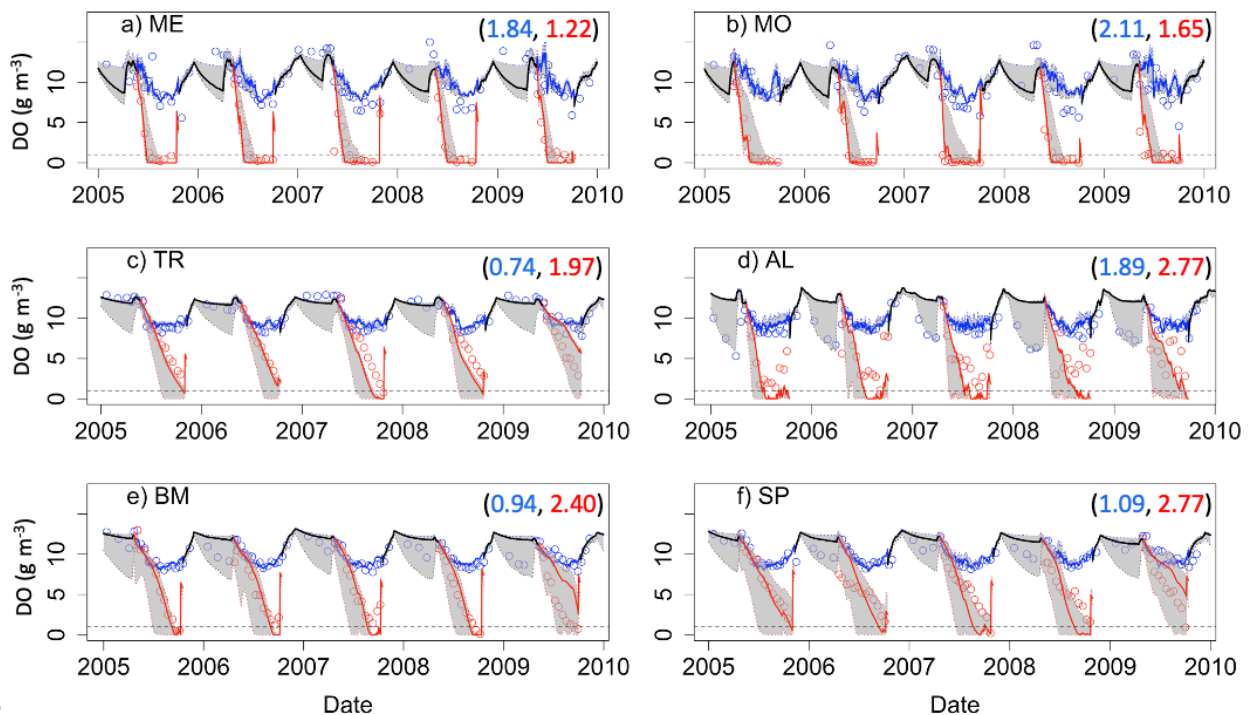
628
629 **Figure 2.** Dissolved oxygen (DO) time series for the years, 2005-2010, for the six study
630 lakes (a-f). Model predictions are represented by lines, and circles represent the observational
631 data. Epilimnetic DO values are blue and Hypolimnetic DO values are red. Fully mixed
632 periods for the lake are indicated by a single black line. RMSE values (epilimnion,
633 hypolimnion; g m^{-3}) for the validation period are included in the upper right of each panel.
634 Uncertainty is represented by gray shading.

635

636

637 ~~The two southern lakes (ME, MO) have DOC RMSE values equal to or greater than 1.00 g C~~

638 ~~m⁻³, while the RMSE for northern lakes ranges from 0.28 g C m⁻³ (TR) to 0.60 g C m⁻³ (AL)~~

639 ~~(Fig. 3).~~ The two southern lakes (ME, MO) have epilimnetic DOC RMSE values greater than

640 1.00 g C m^{-3}, while the RMSE for northern lakes ranges from 0.41 g C m^{-3} (TR) to 0.70 g C m^{-}

641 ^{3} (AL) (Fig. 3). In the southern lakes, NSE epilimnetic DOC values were below -3.00 and

642 KGE values ranged from -0.29 to -0.32. In the northern lakes, NSE values for DOC ranged

643 between -2.75 (SP) and -0.31 (AL). KGE values ranged from -0.07 (BM) to 0.35 (TR). All

644 NSE and KGE metrics for DOC can be found in SI Table 7. Observational data in both

645 southern lakes indicate a decrease in DOC concentration beginning around 2010, which is

646 largely missed in the model predictions (Fig.3a-b, Supplementary Material: Fig. S2a-b) and

647 cause an overestimation of DOC by about 1-2 g C m^{-3}. However, model predictions converge

648 with observed DOC toward the end of the study period (Supplementary Material: Fig. S2a-

649 b). In AL, the seasonal patterns of modeled DOC are smaller in amplitude than the

650 observational data (Supplementary Material: Fig. S2d).
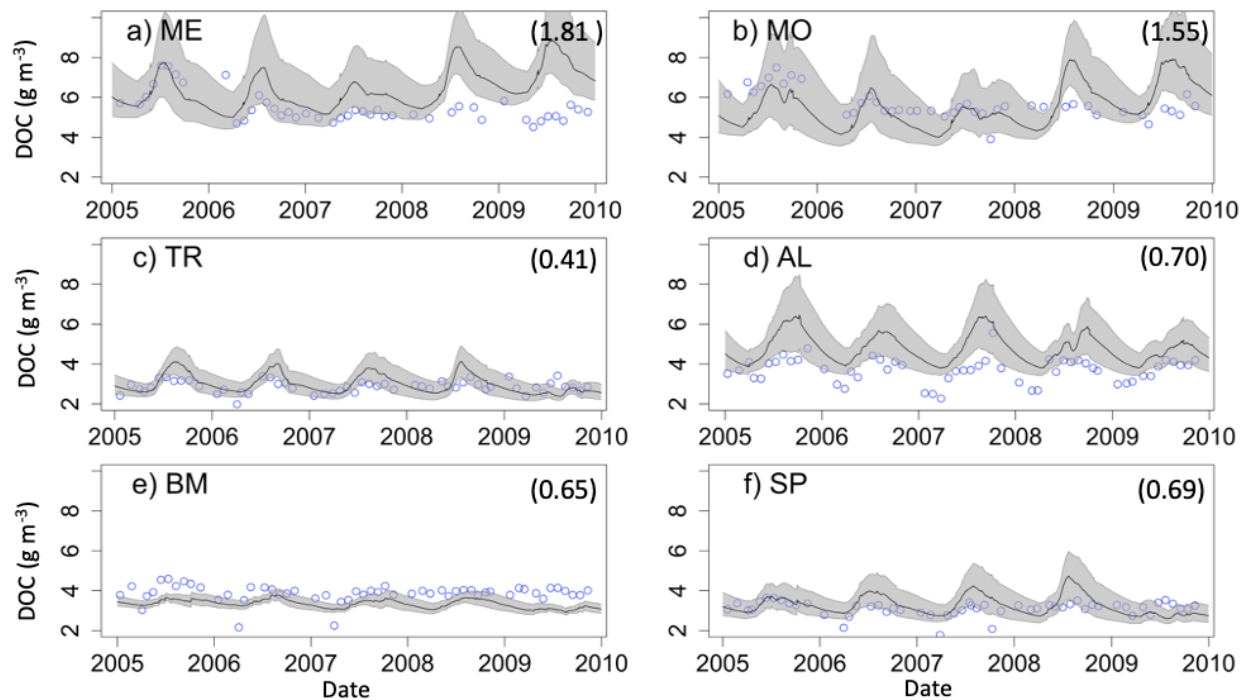
651
652 **Figure 3.** Epilimnetic dissolved organic carbon (DOC) time series for the years, 2005-2010,
653 for the six study lakes (a-f). Model predictions are represented by lines, and circles represent
654 the observational data. RMSE values for the validation period are included for each lake (g C
655 m^{-3}). Uncertainty is represented by gray shading.
656

657 Secchi depth predictions reproduce the mean and seasonal patterns in all lakes (Fig. 4).

658 Although the model produced annual cycles of Secchi depth that generally covered the range

659 of observed values, short term deviations from annual patterns in the observed data are not

660 reproduced. The timing of minima and maxima Secchi depth sometimes differed between

661 predicted and observed values for the northern lakes. In addition, winter extremes in

662 observed Secchi depth are not always reproduced by the model, which is especially evident

663 for ME (Fig. 4a). However, winter observational data for Secchi are more sparse than other

664 seasons.

665
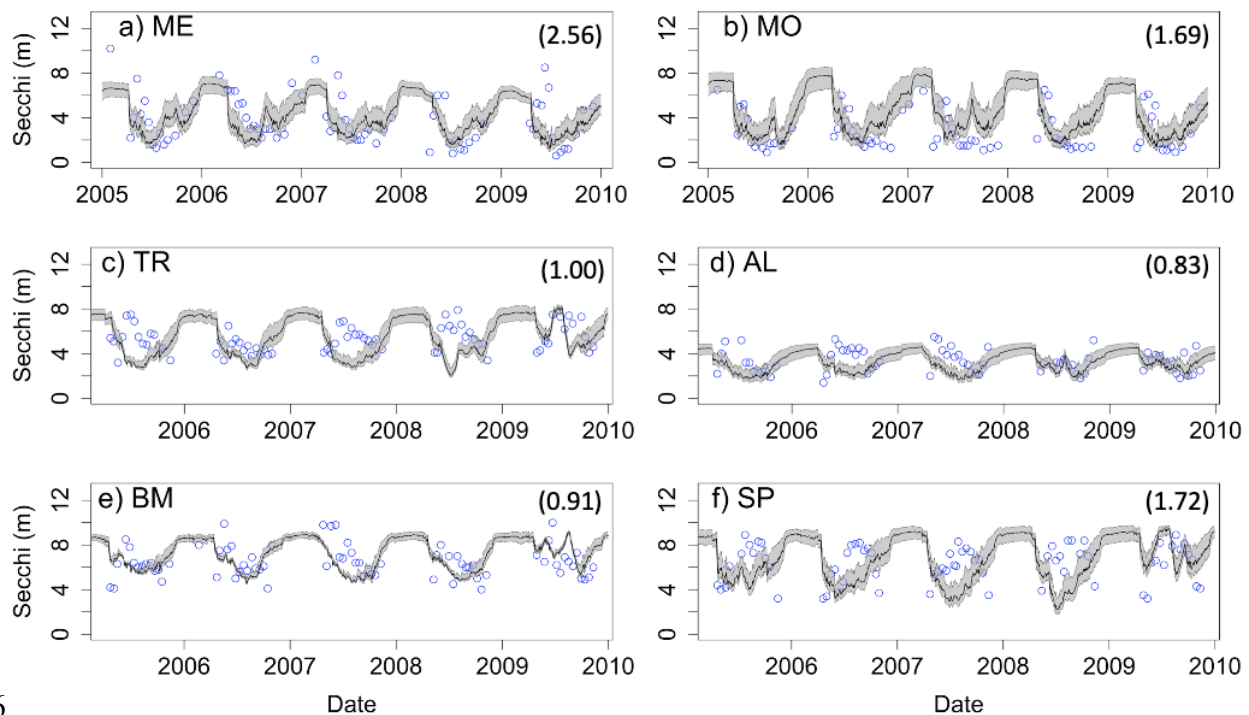
666
667 **Figure 4.** Secchi depth time series for the years, 2005-2010, for the six study lakes (a-f).
668 Model predictions are represented by lines, and circles represent the observational data.
669 RMSE values for the validation period are included for each lake (m). Uncertainty is
670 represented by gray shading.
671

672

673 **3.2 Ecosystem Processes**

674 The mean annual OC budgets of all six lakes show large differences in the sources and fates

675 of OC among lakes (Fig. 5; Supplementary Material: Table S3). Autochthony is the dominant

676 source of OC for all study lakes. Water column respiration is the largest portion of whole-

677 lake respiration in ME, MO, TR, SP, and BM. Sediment respiration contributions are a lower

678 proportion of total respiration in ME, MO, and TR (mean of ~~15.0%~~ 14.1%), and are slightly

679 higher in BM and SP (mean of ~~23.7%~~ 18.7%). AL has a more even distribution of OC fates.

680 OC burial amounts also vary across the study lakes, with the highest percentage in AL

681 (~~26.4%~~ 34.1%), and lowest in SP (~~2.5%~~ 5.25%).

682
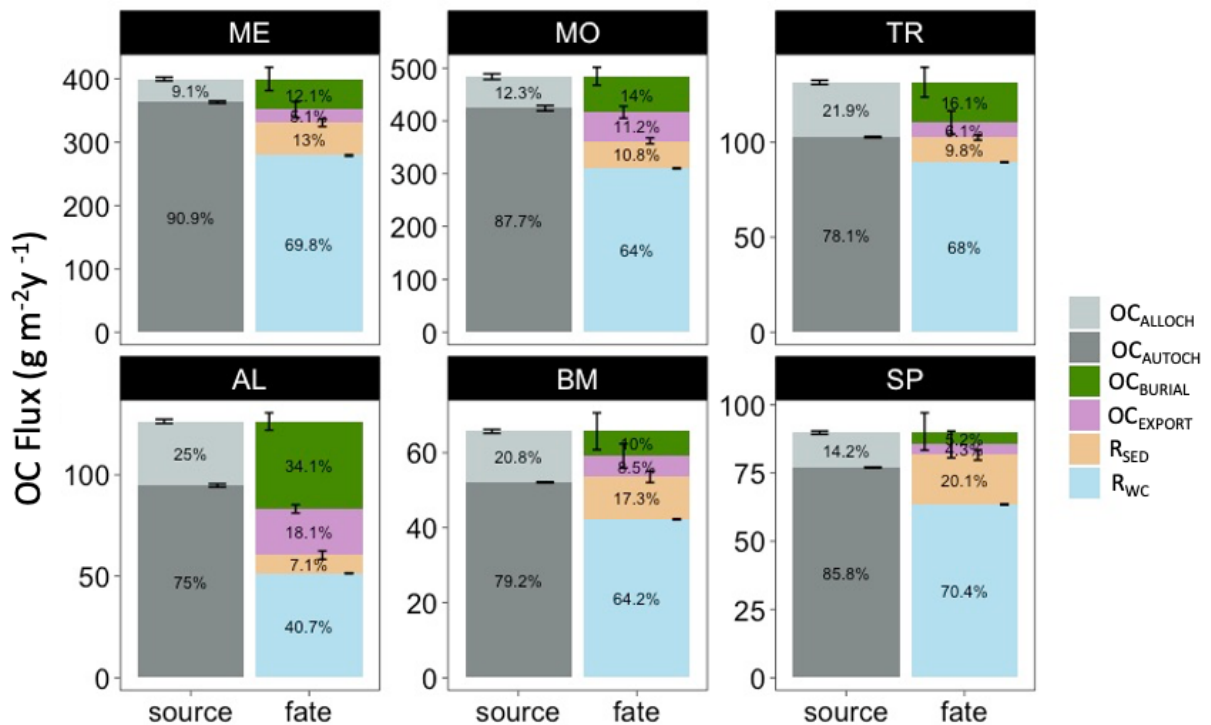
683
Figure 5. Total annual budget, sources (left stacked bars) and fates (right stacked bars), of
organic carbon (OC) in each lake over the study period. The OC sources include
allochthonous OC (OC_{ALLOCH}) and autochthonous OC (OC_{AUTOCH}). The OC fates include
burial of OC (OC_{BURIAL}), export of OC (OC_{EXPORT}), sediment respiration of OC (R_{SED}), and
water column respiration of OC (R_{WC}). Standard error bars for the annual means are
indicated for each source and fate as well. Note that the magnitudes of the y-axis differ
among the lakes. A significance test comparing these fluxes across the study lakes can be
found in SI Table 6.

692

693   The lakes show inter-annual variation in trophic state, as quantified by NEP (Fig. 6). Total

694   respiration (water column and sediment) exceeds autochthony in SP, BM, and TR, indicating

695   predominantly net heterotrophy for these systems. The remaining lakes (ME, MO, AL) are

696   generally net autotrophic. The southern lakes (ME, MO) are net autotrophic (positive NEP)

697   for the majority of the study years but became less autotrophic over the last five years of the

698   study period (2010-2014). BM and SP are mostly net heterotrophic (negative NEP) over the

699   study period with a few brief instances of net autotrophy. The strongest autotrophic signal for

700   these lakes occurred around 2010. TR experienced prolonged periods of both autotrophy and

701   heterotrophy. AL is net autotrophic over the study period but had lower average NEP than

702   the southern lakes. ME, MO, and AL all have negative trends in NPP, but only ME and AL

703   were ~~was~~ significant (p_value < 0.1, Mann-Kendall test) (SI Table 2). Of these three lakes,

704   ME and AL also have decreasing significant trends in annual total phosphorus concentration

705   (SI Table 2). No significant trends were found for NPP or total phosphorus in the other lakes

706   (MO, TR, BM, SP).
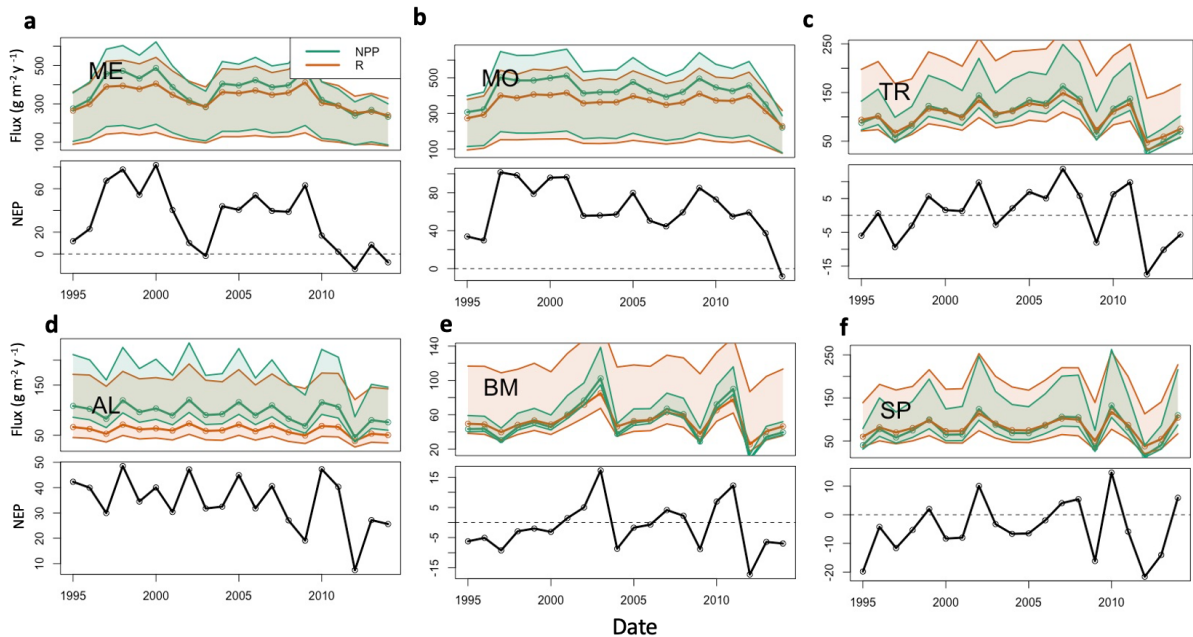
707
708 **Figure 6.** Time series of calibrated lake Net Primary Production (green), Total Respiration
709 (red) (top panels), and Net Ecosystem Production (NEP, bottom panels) for the six lakes: (a)
710 Lake Mendota; (b) Lake Monona; (c) Trout Lake; (d) Allequash Lake; (e) Big Muskellunge
711 Lake, and; (f) Sparkling Lake. Fluxes are in units of $gC\,m^{-2}y^{-1}$. Solid line represents
712 prediction based on best parameter estimates. Shaded regions represent prediction
713 uncertainty based on parameter ranges in Table 3. Shaded region for NEP not shown to
714 reduce axis limits and emphasize NEP pattern.

715
716

717   Hypolimnetic DO consumption during stratified periods was modeled as a function of the

718   two components of hypolimnetic respiration, hypolimnetic water column respiration and

719   hypolimnetic sediment respiration. Water column respiration contributes more than sediment

720   respiration to total hypolimnetic respiration in the southern lakes compared to the northern

721   lakes, with the exception of TR, where cumulative water column respiration is much larger

722   than cumulative sediment respiration. In ME and MO, the mass of summer autochthonous

723   POC entering the hypolimnion is similar to the total hypolimnetic OC mass respired for the

724   beginning of the stratified period (Fig. 7a-b; green line). Later in the stratified period, an

725   increase in epilimnetic POC and associated settling exceeds total hypolimnetic respiration

726   (Fig. 7a-b; green hashed area). This is due, in part, to lower respiration rates that occur once

727   DO (gray line) has been fully depleted, which occurs in early July for ME and late June for

728   MO. In BM and SP the total hypolimnetic respiration slightly exceeds autochthonous POC

729   inputs during parts of the stratified period, indicating the importance of allochthony in these

730   systems (Fig. 7c,f). BM shows that autochthonous POC entering the hypolimnion and total

731   hypolimnetic respiration are similar for much of the stratified period (Fig. 7d). AL is the only

732   lake to have autochthonous POC inputs consistently larger than total hypolimnetic respiration

733   during the stratified season. All lakes show that summer allochthonous POC entering the

734   hypolimnion is a small contribution to the overall hypolimnetic POC load.

735
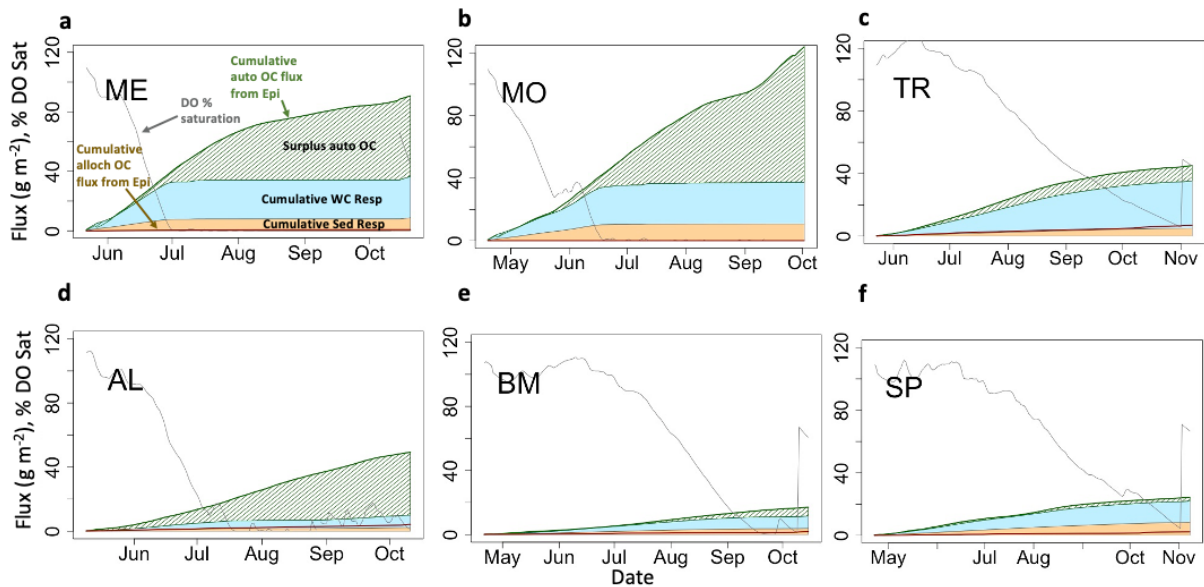
736
737 **Figure 7.** Hypolimnetic dissolved oxygen, allochthonous (alloch) and autochthonous (auto)
738 organic carbon loading, and respiration dynamics during one stratified period (2005) for each
739 lake. Fluxes are cumulative $gC\ m^{-2}$ and DO is presented as percent saturation. Labels are in
740 panel (a). Note that the cumulative water column (WC) and sediment (Sed) respiration fluxes
741 are stacked, while other cumulative fluxes are not.
742

743 Respiration of autochthonous POC and sediment respiration account for most of the total

744 hypolimnetic respiration in all lakes (Fig. 8). Respiration of DOC accounts for a relatively

745 small proportion of total respiration. Total hypolimnetic respiration is higher in the southern

746 lakes than the northern lakes. TR has the highest amount of hypolimnetic respiration for the

747 northern lakes, and AL and BM have the least amounts of hypolimnetic respiration. ~~Water~~

748 ~~column respiration contributed the most towards total hypolimnetic respiration in ME, MO,~~

749 ~~and TR. Sediment respiration and water column respiration contributed similar proportions~~

750 ~~towards total hypolimnetic respiration in BM, SP, and AL. As total respiration across lakes~~

751 ~~increases, a larger proportion of that respiration is attributable to respiration of POC in the~~

752 ~~water column. DOC water column respiration was the smallest proportion of total~~

753 ~~hypolimnetic respiration in all six study lakes.~~ Water column respiration contributed the most

754 towards total hypolimnetic respiration in all lakes. Sediment respiration contributed the

755 largest proportion towards total hypolimnetic respiration in BM and SP. DOC water column

756 respiration was the smallest proportion of total hypolimnetic respiration in all six study lakes.
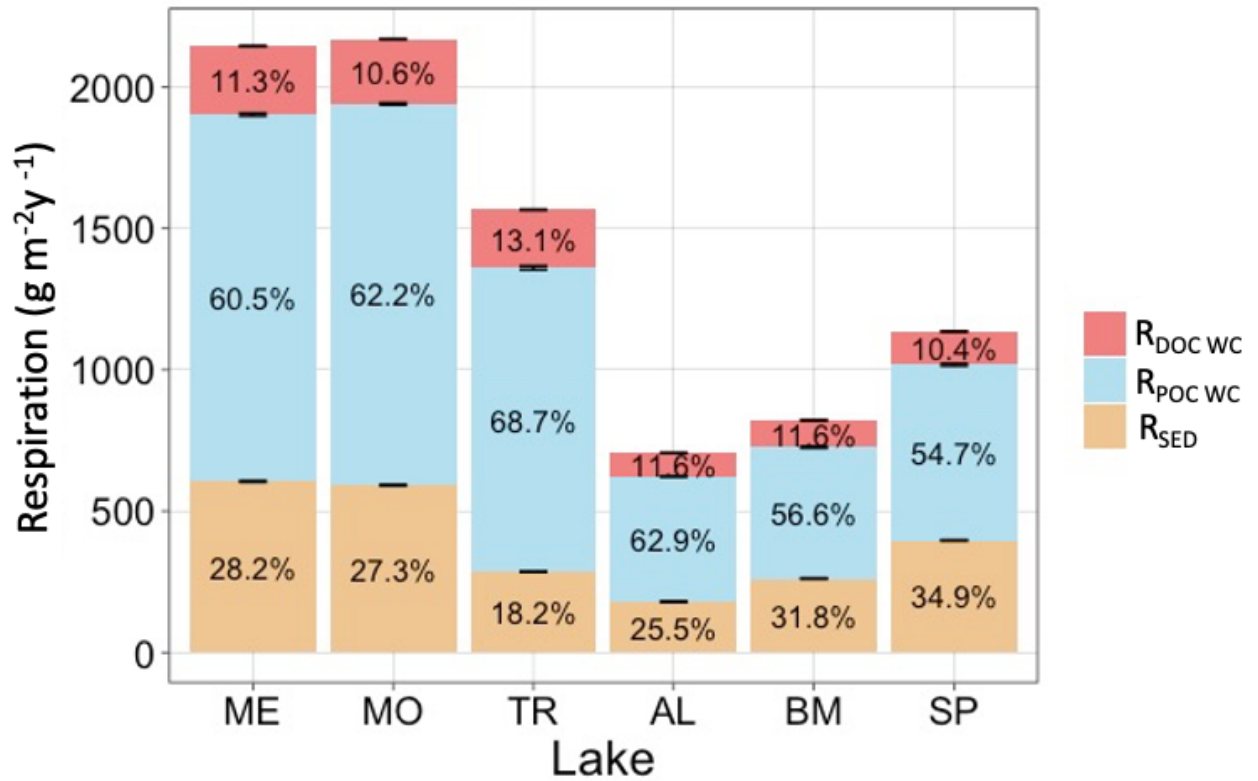
757
758 **Figure 8.** Total average annual hypolimnetic respiration, separated by percentages attributed
759 to water column DOC ($R_{DOC\ WC}$), water column POC ($R_{POC\ WC}$), and sediment (R_{SED}) organic
760 carbon sources. Standard error bars for the annual respiration values are indicated as well.
761

762

763

764 **4 Discussion**

765

766 **4.1 Autochthonous and Allochthonous Loads**

767 Autochthony was the dominant source of OC subsidizing hypolimnetic respiration in the

768 study lakes. The importance of autochthonous OC pools in ecosystem respiration was

769 surprising, given ample research highlighting the dominance of allochthonous OC in north

770 temperate lakes (Wilkinson et al. 2013; Hanson et al. 2011; Hanson et al. 2014). This

771 outcome emphasizes the utility of process-based models in studying mechanisms that discern

772 the relative contributions of different pools of organic matter to lake metabolism.

773 Autochthonous OC pools have higher turnover rates than allochthonous OC pools (Dordoni

774 et al., 2022) and often are lower in concentration than the more recalcitrant allochthonous

775 pools (Wilkinson et al. 2013). Thus, studies based on correlative relationships between lake

776 concentrations of organic matter and water quality metrics, likely overlook the importance of

777 more labile organic matter in driving observable ecosystem phenomena, such as gas flux and

778 formation of hypolimnetic anoxia (Evans et al., 2005; Feng et al., 2022). By quantifying

779 metabolism fluxes relevant to both OC pools, we can recreate shorter-term OC processes that

780 quantify high turnover of labile organic matter, which would typically be missed by

781 empirical studies based on monthly or annual observations.

782

783 Allochthony and autochthony are important to lake carbon cycling, but in ways that play out

784 at different time scales. Allochthonous OC has been well-established as an important factor

785 in driving negative NEP through a number of mechanisms (Wilkinson et al., 2013; Hanson et

786 al., 2014; Hanson et al., 2011). Allochthony contributes to water quality variables, such as

787 Secchi depth (Solomon et al. 2015), by providing the bulk of DOC in most lakes (Wilkinson

788 et al., 2013) and can drive persistent hypolimnetic anoxia in dystrophic lakes (Knoll et al.,

789   2018). In contrast, autochthony contributes to seasonal dynamics of water quality through

790   rapid changes in OC that can appear and disappear within a season. Within that seasonal time

791   frame, autochthonous POC settling from the epilimnion can drive hypolimnetic respiration,

792   thus controlling another key water quality metric, oxygen depletion. It is worth noting that

793   our model does not discern allochthonous and autochthonous sediment OC, however we

794   show that autochthonous OC makes up the largest proportion of OC loads in our study lakes

795   and therefore autochthony likely contributes substantially to the sediment OC pool. For

796   highly eutrophic lakes, the model results show excess autochthony stored in the sediments

797   which may carry into subsequent years, potentially providing additional substrate for

798   sediment respiration. Thus, understanding and predicting controls over hypolimnetic oxygen

799   depletion benefits from quantifying both allochthonous and autochthonous OC cycles.

800

801   Differences in trophic status, hydrologic residence time, and inflow sources help explain the

802   relative proportion of allochthonous versus autochthonous OC among lakes in our study.

803   Water residence times (Hotchkiss et al. 2018; McCullough et al. 2018) and surrounding land

804   cover (Hanson et al. 2014) have been shown to have a substantial impact on OC dynamics by

805   controlling allochthonous OC loading and NEP trends on lakes included in our study

806   (Hanson et al. 2014, McCullough et al. 2018). We built upon these ideas by recreating daily

807   watershed loading dynamics of POC and DOC from derived discharge data and incorporating

808   nutrient control over lake primary production by using high quality and long-term

809   observational data. The northern lakes are embedded in a forest and wetland landscape,

810   which are characteristic of having higher DOC than the urban and agricultural landscape of

811   the southern lakes (Creed et al., 2003). This creates variation in allochthonous loading across

812   the study lakes. Lake trophic state and productivity are a major control for autochthonous

813   production, which influences autochthonous loads across the study lakes as well. For lake

814   metrics that are comparable between studies, such as allochthonous loading and export,

815   allochthonous water column respiration, and total OC burial, our results were within 20% of

816   values in related studies (Hanson et al. 2014, McCullough et al. 2018).

817

818   **4.2 Hypolimnetic Respiration**

819   Given the importance of autochthonous POC to hypolimnetic respiration, we assume it

820   contributes substantially to both sediment respiration and respiration in the water column.

821   While previous work found that sediment respiration was the dominant respiration source for

822   lakes with depth ranges encompassed within our study (Steinsberger 2020), we found that

823   water column respiration was at least as important, if not more so. Differences in these

824   findings could be linked to uncertainty in the settling velocity of POC, due to lack of

825   empirical POC settling velocity measurements. Perhaps, POC mineralized in the hypolimnia

826   of our modeled lakes passes more quickly to the sediments in real ecosystems, shifting the

827   balance of respiration more toward the sediments. ~~It has been shown that POC respiration~~

828   ~~contributes substantially to hypolimnetic DO depletion (Jenny et al. 2016)~~ OC respiration can

829   contribute substantially to hypolimnetic DO depletion in both lakes and reservoirs (Beutel,

830   2003), and POC settling velocities can be highly variable, suggesting that assumptions

831   around vertical distribution of lake POC deserve further investigation. Another possible

832   explanation for these differences could be that our model missed allochthonous POC loads

833   from extreme events (Carpenter et al., 2012), which can increase the amount of legacy OC

834   stored in the sediments and increase sediment respiration. Our model also does not account

835   for reduced respiration rates due to OC aging, which may explain our higher values of water

836   column respiration. Finally, our model includes entrainment as a possible oxygen source to

837   the hypolimnion, which must be offset by respiration to fit observed hypolimnetic DO

838   changes. Any study that underestimates DO sources to the hypolimnion likely underestimates

839   total respiration.

840

841   Anaerobic mineralization of organic carbon is an important biogeochemical process and can

842   be a substantial carbon sink through methanogenesis (Maerki et al. 2009). Although

843   methanogenesis is not incorporated into our model, methane dissolved in the water column of

844   Lake Mendota is mostly oxidized (Hart 2017), thus contributing to the overall oxygen

845   demand, which is accounted for in our model. What remains unaccounted is ebullition of

846   methane, which is a carbon flux that is difficult to quantify (McClure et al. 2020). Future

847   metabolism studies that include these processes might find a decrease in annual OC burial

848   rates relative to rates in our study. Although we believe that ebullition is not a substantial

849   portion of the lake's carbon mass budget, that remains to be studied more carefully. As the

850   model accounts for DO consumption through calibration, the overall flux would not change

851   even if we link DO consumption to methane oxidation, only the process description would be

852   more realistic.

853

854 ~~Finally, our model includes entrainment as a possible oxygen source to the hypolimnion,~~

855 ~~which must be offset by respiration to fit observed hypolimnetic DO changes. Any study that~~

856 ~~underestimates DO sources to the hypolimnion likely underestimates total respiration.~~ Our

857 findings highlight the importance of autochthonous POC in hypolimnetic oxygen depletion

858 and suggest that related processes, such as the timing of nutrient loading, changes in

859 thermocline depth, or zooplankton grazing, could impact overall lake respiration dynamics

860 and anoxia formation (Schindler et al., 2016; Ladwig et al., 2021; Müller et al., 2012).

861

862 **4.3 Long-term Dynamics**

863 Although autochthonous OC dominated the loads across the study lakes, analysis of the long-

864 term OC dynamics supports the importance of allochthony in lakes. Net Ecosystem

865 Production (NEP) has been used to quantify heterotrophy and autotrophy in lakes (Odum

866 1956, Hanson et al. 2003, Cole et al. 2000, Lovett et al. 2006), and using this metric over

867 multiple decades allowed us to analyze long-term impacts of allochthony. TR, BM, and SP

868 fluctuated between heterotrophy and autotrophy, usually in tandem with trends in hydrology,

869 which acts as a main control of allochthonous OC. This suggests that allochthonous OC

870 inputs may be less important for seasonal anoxia but can still drive a lake toward negative

871 NEP and contribute to sediment carbon storage over long time periods. ME, MO, and AL

872 tended to become less autotrophic over time (Fig. 6), a pattern that coincided with significant

873 decreasing trends in mean epilimnetic total phosphorus concentrations for ME and AL (SI

874 Fig. 5). In our model, NPP and phosphorus are directly related, so decreases in phosphorus

875 are likely to cause decreases in NEP. Short-term respiration of autochthonous POC can

876 account for rapid decreases in hypolimnetic DO, but allochthonous POC, which tends to be

877 more recalcitrant, provides long-term subsidy of ecosystem respiration that can result in

878 long-term net heterotrophy. Thus, it's critical to understand and quantify both the rapid

879 internal cycling based on autochthony and the long and slow turnover of allochthony.

880

881 Through explicitly simulating the cycling of both allochthony and autochthony, we can

882 expand our conceptual model of metabolism to better understand time dynamics of lake

883 water quality at the ecosystem scale. Autochthony has pronounced seasonal dynamics,

884 typically associated with the temporal variability of phytoplankton communities and the

885 growth and senescence of macrophytes (Rautio et al., 2011). While allochthony can also have

886 strong seasonal patterns associated with leaf litter input, pollen blooms, and spring runoff

887 events, its more recalcitrant nature leads to a less pronounced seasonal signal at the

888 ecosystem scale (Wilkinson et al., 2013, Tranvik 1998). When considered together, it seems

889 that allochthony underlies long and slow changes in metabolism patterns, while autochthony

890 overlays strong seasonality. Both OC pools are important for ecosystem scale metabolism

891 processes, and their consequences are evident at different time scales. Therefore, the

892 interactions of both OC sources and their influences on water quality patterns deserve further

893 investigation.

894

895 Autochthonous OC control over hypolimnetic respiration should be a primary consideration

896 for understanding the influence of OC on ecosystem dynamics. Hypolimnetic oxygen

897 depletion and anoxia in productive lakes can be mitigated by reducing autochthonous

898   production of OC, which we show is mainly driven by nutrient availability. This study also

899   identifies the need for a better understanding of internal and external OC loads in lakes.

900   Previous studies have found heterotrophic behavior in less productive lakes, but our findings

901   highlight the importance of autochthony in these lakes, especially for shorter-time scale

902   processes that can be missed by looking at broad annual patterns. By using a one-

903   dimensional, two-layer model, we are able to also understand how surface metabolism

904   processes can impact bottom layer dynamics, which would not be possible with a zero-

905   dimensional model. Looking forward, we believe that our understanding of these processes

906   could be improved by building a coupled watershed - metabolism model to more closely

907   explore causal relations between watershed hydrology, nutrient dynamics, and lake

908   morphometry.

909

910

911

912 *Code Availability*
913 Model code and figure creation code are archived in the Environmental Data Initiative
914 repository (https://doi.org/10.6073/PASTA/1B5B947999AA2F9E0E95C91782B36EE9,
915 Delany, 2022).
916
917 *Data Availability*
918 Driving data, model configuration files, and model result data are archived in the
919 Environmental Data Initiative repository
920 (https://doi.org/10.6073/PASTA/1B5B947999AA2F9E0E95C91782B36EE9, Delany, 2022).
921
922 *Author Contributions*
923 AD, PH, RL, and CB assisted with model development and analysis of results. AD and PH
924 prepared the manuscript with contributions from RL, CB, and EA.
925
926 *Competing Interests*
927 The authors declare that they have no conflict of interest.
928
929 *Acknowledgements:*
930 Funding was provided through the National Science Foundation (NSF), with grants DEB-
931 1753639, DEB-1753657, and DEB-2025982. Funding for Ellen Albright was provided by the
932 NSF Graduate Research Fellowship Program (GRFP), and the Iowa Department of Natural
933 Resources (contract #22CRDLWBMBALM-0002). Funding for Robert Ladwig was
934 provided by the NSF ABI development grant (#DBI 1759865), UW-Madison Data Science
935 Initiative grant, and the NSF HDR grant (#1934633). Data were provided by the North
936 Temperate Lakes Long Term Ecological Research Program and was accessed through the
937 Environmental Data Initiative (DOI: 10.6073/pasta/0dbbfdbcdee623477c000106c444f3fd).
938

939 References

940 Amon, R. M. W., & Benner, R. (1996). Photochemical and microbial consumption of

941   dissolved organic carbon and dissolved oxygen in the Amazon River system.

942   *Geochimica et Cosmochimica Acta*, *60*(10), 1783–1792. https://doi.org/10.1016/0016-

943   7037(96)00055-5

944 Beutel, M. W. (2003). Hypolimnetic Anoxia and Sediment Oxygen Demand in California

945   Drinking Water Reservoirs. *Lake and Reservoir Management*, *19*(3), 208–221.

946   https://doi.org/10.1080/07438140309354086

947 Bryant, L. D., Hsu-Kim, H., Gantzer, P. A., & Little, J. C. (2011). Solving the problem at the

948   source: Controlling Mn release at the sediment-water interface via hypolimnetic

949   oxygenation. *Water Research*, *45*(19), 6381–6392.

950   https://doi.org/10.1016/j.watres.2011.09.030

951 Cardille, J. A., Carpenter, S. R., Coe, M. T., Foley, J. A., Hanson, P. C., Turner, M. G., &

952   Vano, J. A. (2007). Carbon and water cycling in lake-rich landscapes: Landscape

953   connections, lake hydrology, and biogeochemistry. *Journal of Geophysical Research*,

954   *112*(G2), G02031. https://doi.org/10.1029/2006JG000200

955 Carpenter, S., Arrow, K., Barrett, S., Biggs, R., Brock, W., Crépin, A.-S., Engström, G.,

956   Folke, C., Hughes, T., Kautsky, N., Li, C.-Z., McCarney, G., Meng, K., Mäler, K.-G.,

957   Polasky, S., Scheffer, M., Shogren, J., Sterner, T., Vincent, J., … Zeeuw, A. (2012).

958   General Resilience to Cope with Extreme Events. *Sustainability*, *4*(12), 3248–3259.

959   https://doi.org/10.3390/su4123248

960 Carpenter, S. R., Benson, B. J., Biggs, R., Chipman, J. W., Foley, J. A., Golding, S. A.,

961   Hammer, R. B., Hanson, P. C., Johnson, P. T. J., Kamarainen, A. M., Kratz, T. K.,

962   Lathrop, R. C., McMahon, K. D., Provencher, B., Rusak, J. A., Solomon, C. T., Stanley,

963   E. H., Turner, M. G., Vander Zanden, M. J., … Yuan, H. (2007). Understanding

964   Regional Change: A Comparison of Two Lake Districts. *BioScience*, *57*(4), 323–335.

965   https://doi.org/10.1641/B570407

966 Catalán, N., Marcé, R., Kothawala, D. N., & Tranvik, Lars. J. (2016). Organic carbon

967   decomposition rates controlled by water retention time across inland waters. *Nature*

968   *Geoscience*, *9*(7), 501–504. https://doi.org/10.1038/ngeo2720

969 Cole, G., & Weihe, P. (2016). *Textbook of Limnology*. Waveland Press, Inc.

970 Cole, J. J., & Caraco, N. F. (1998). Atmospheric exchange of carbon dioxide in a low-wind

971   oligotrophic lake measured by the addition of SF_6. *Limnology and Oceanography*,

972   *43*(4), 647–656. https://doi.org/10.4319/lo.1998.43.4.0647

973 Cole, J. J., Carpenter, S. R., Kitchell, J. F., & Pace, M. L. (2002). Pathways of organic carbon

974   utilization in small lakes: Results from a whole-lake ^{13}C addition and coupled model.

975   *Limnology and Oceanography*, *47*(6), 1664–1675.

976   https://doi.org/10.4319/lo.2002.47.6.1664

977 Cole, J. J., Pace, M. L., Carpenter, S. R., & Kitchell, J. F. (2000). Persistence of net

978   heterotrophy in lakes during nutrient addition and food web manipulations. *Limnology*

979   *and Oceanography*, *45*(8), 1718–1730. https://doi.org/10.4319/lo.2000.45.8.1718

980

981   Creed, I. F., Sanford, S. E., Beall, F. D., Molot, L. A., & Dillon, P. J. (2003). Cryptic

982   wetlands: Integrating hidden wetlands in regression models of the export of dissolved

983   organic carbon from forested landscapes. *Hydrological Processes*, *17*(18), 3629–3648.

984   https://doi.org/10.1002/hyp.1357

985   Delany, A. (2022). *Modeled Organic Carbon, Dissolved Oxygen, and Secchi for six*

986   *Wisconsin Lakes, 1995-2014* [Data set]. Environmental Data Initiative.

987   https://doi.org/10.6073/PASTA/1B5B947999AA2F9E0E95C91782B36EE9

988   Dordoni, M., Seewald, M., Rinke, K., van Geldern, R., Schmidmeier, J., & Barth, J. A. C.

989   (2022). *Mineralization of autochthonous particulate organic carbon is a fast channel of*

990   *organic matter turnover in Germany's largest drinking water reservoir* [Preprint].

991   Biogeochemistry: Stable Isotopes & Other Tracers. https://doi.org/10.5194/bg-

992   2022-154

993   Evans, C. D., Monteith, D. T., & Cooper, D. M. (2005). Long-term increases in surface water

994   dissolved organic carbon: Observations, possible causes and environmental impacts.

995   *Environmental Pollution*, *137*(1), 55–71. https://doi.org/10.1016/j.envpol.2004.12.031

996   Feng, L., Zhang, J., Fan, J., Wei, L., He, S., & Wu, H. (2022). Tracing dissolved organic

997   matter in inflowing rivers of Nansi Lake as a storage reservoir: Implications for water-

998   quality control. *Chemosphere*, *286*, 131624.

999   https://doi.org/10.1016/j.chemosphere.2021.131624

1000

1001

1002 Goudsmit, G.-H., Burchard, H., Peeters, F., & Wüest, A. (2002). Application of k-ϵ

1003   turbulence models to enclosed basins: The role of internal seiches: APPLICATION OF

1004   k-ϵ TURBULENCE MODELS. *Journal of Geophysical Research: Oceans*, *107*(C12),

1005   23-1-23–13. https://doi.org/10.1029/2001JC000954

1006 Hanson, P. C., Bade, D. L., Carpenter, S. R., & Kratz, T. K. (2003). Lake metabolism:

1007   Relationships with dissolved organic carbon and phosphorus. *Limnology and*

1008   *Oceanography*, *48*(3), 1112–1119. https://doi.org/10.4319/lo.2003.48.3.1112

1009 Hanson, P.C., Carpenter S.R., Cardille, J.A, Coe, M.T., & Winslow, L.A. (2007). Small lakes

1010   dominate a random sample of reginal lake characteristics. *Freshwater Biology* 52(5),

1011   814–822. https://doi.org/10.1111/j.1365-2427.2007.01730.x

1012 Hanson, P. C., Buffam, I., Rusak, J. A., Stanley, E. H., & Watras, C. (2014). Quantifying lake

1013   allochthonous organic carbon budgets using a simple equilibrium model. *Limnology and*

1014   *Oceanography*, *59*(1), 167–181. https://doi.org/10.4319/lo.2014.59.1.0167

1015 Hanson, P. C., Hamilton, D. P., Stanley, E. H., Preston, N., Langman, O. C., & Kara, E. L.

1016   (2011). Fate of Allochthonous Dissolved Organic Carbon in Lakes: A Quantitative

1017   Approach. *PLoS ONE*, *6*(7), e21884. https://doi.org/10.1371/journal.pone.0021884

1018 Hanson, P. C., Pace, M. L., Carpenter, S. R., Cole, J. J., & Stanley, E. H. (2015). Integrating

1019   Landscape Carbon Cycling: Research Needs for Resolving Organic Carbon Budgets of

1020   Lakes. *Ecosystems*, *18*(3), 363–375. https://doi.org/10.1007/s10021-014-9826-9

1021 Hanson, P. C., Pollard, A. I., Bade, D. L., Predick, K., Carpenter, S. R., & Foley, J. A.

1022   (2004). A model of carbon evasion and sedimentation in temperate lakes:

LANDSCAPE-LAKE CARBON CYCLING MODEL. *Global Change Biology*, *10*(8), 1285–1298. https://doi.org/10.1111/j.1529-8817.2003.00805.x

Hanson, P. C., Stillman, A. B., Jia, X., Karpatne, A., Dugan, H. A., Carey, C. C., Stachelek, J., Ward, N. K., Zhang, Y., Read, J. S., & Kumar, V. (2020). Predicting lake surface water phosphorus dynamics using process-guided machine learning. *Ecological Modelling*, *430*, 109136. https://doi.org/10.1016/j.ecolmodel.2020.109136

Hart, J., Dugan, H., Carey, C., Stanley, E., & Hanson, P. (2019). *Lake Mendota Carbon and Greenhouse Gas Measurements at North Temperate Lakes LTER 2016* [Data set]. Environmental Data Initiative. https://doi.org/10.6073/PASTA/170E5BA0ED09FE3D5837EF04C47E432E

Hipsey, M. R. (2022). *Modelling Aquatic Eco-Dynamics: Overview of the AED modular simulation platform*. https://doi.org/10.5281/ZENODO.6516222

Hipsey, M. R., Bruce, L. C., Boon, C., Busch, B., Carey, C. C., Hamilton, D. P., Hanson, P. C., Read, J. S., de Sousa, E., Weber, M., & Winslow, L. A. (2019). A General Lake Model (GLM 3.0) for linking with high-frequency sensor data from the Global Lake Ecological Observatory Network (GLEON). *Geoscientific Model Development*, *12*(1), 473–523. https://doi.org/10.5194/gmd-12-473-2019

Hoffman, A. R., Armstrong, D. E., & Lathrop, R. C. (2013). Influence of phosphorus scavenging by iron in contrasting dimictic lakes. *Canadian Journal of Fisheries and Aquatic Sciences*, *70*(7), 941–952. https://doi.org/10.1139/cjfas-2012-0391

1044   Hotchkiss, E. R., Sadro, S., & Hanson, P. C. (2018). Toward a more integrative perspective

1045   on carbon metabolism across lentic and lotic inland waters. *Limnology and*

1046   *Oceanography Letters*, *3*(3), 57–63. https://doi.org/10.1002/lol2.10081

1047   Houser, J. N., Bade, D. L., Cole, J. J., & Pace, M. L. (2003). The dual influences of dissolved

1048   organic carbon on hypolimnetic metabolism: Organic substrate and photosynthetic

1049   reduction. *Biogeochemistry*, *64*(2), 247–269. https://doi.org/10.1023/A:1024933931691

1050   Hunt, R. J., & Walker, J. F. (2017). *2016 Update to the GSFLOW groundwater-surface water*

1051   *model for the Trout Lake Watershed*. https://doi.org/10.5066/F7M32SZ2

1052   Hunt, R. J., Walker, J. F., Selbig, W. R., Westenbroek, S. M., & Regan, R. S. (2013).

1053   *Simulation of Climate-Change Effects on Streamflow, Lake Water Budgets, and Stream*

1054   *Temperature Using GSFLOW and SNTEMP, Trout Lake Watershed, Wisconsin*. United

1055   States Geological Survey.

1056   Jane, S. F., Hansen, G. J. A., Kraemer, B. M., Leavitt, P. R., Mincer, J. L., North, R. L., Pilla,

1057   R. M., Stetler, J. T., Williamson, C. E., Woolway, R. I., Arvola, L., Chandra, S.,

1058   DeGasperi, C. L., Diemer, L., Dunalska, J., Erina, O., Flaim, G., Grossart, H.-P.,

1059   Hambright, K. D., … Rose, K. C. (2021). Widespread deoxygenation of temperate lakes.

1060   *Nature*, *594*(7861), 66–70. https://doi.org/10.1038/s41586-021-03550-y

1061   Jansson, M., Bergström, A.-K., Blomqvist, P., & Drakare, S. (2000). ALLOCHTHONOUS

1062   ORGANIC CARBON AND PHYTOPLANKTON/BACTERIOPLANKTON

1063   PRODUCTION RELATIONSHIPS IN LAKES. *Ecology*, *81*(11), 3250–3255.

1064   https://doi.org/10.1890/0012-9658(2000)081[3250:AOCAPB]2.0.CO;2

1065   Jenny, J.-P., Francus, P., Normandeau, A., Lapointe, F., Perga, M.-E., Ojala, A.,

1066   Schimmelmann, A., & Zolitschka, B. (2016). Global spread of hypoxia in freshwater

1067   ecosystems during the last three centuries is caused by rising local human pressure.

1068   *Global Change Biology*, *22*(4), 1481–1489. https://doi.org/10.1111/gcb.13193

1069   Jenny, J.-P., Normandeau, A., Francus, P., Taranu, Z. E., Gregory-Eaves, I., Lapointe, F.,

1070   Jautzy, J., Ojala, A. E. K., Dorioz, J.-M., Schimmelmann, A., & Zolitschka, B. (2016).

1071   Urban point sources of nutrients were the leading cause for the historical spread of

1072   hypoxia across European lakes. *Proceedings of the National Academy of Sciences*,

1073   *113*(45), 12655–12660. https://doi.org/10.1073/pnas.1605480113

1074   Knoll, L. B., Williamson, C. E., Pilla, R. M., Leach, T. H., Brentrup, J. A., & Fisher, T. J.

1075   (2018). Browning-related oxygen depletion in an oligotrophic lake. *Inland Waters*, *8*(3),

1076   255–263. https://doi.org/10.1080/20442041.2018.1452355

1077   Kraemer, B. M., Chandra, S., Dell, A. I., Dix, M., Kuusisto, E., Livingstone, D. M.,

1078   Schladow, S. G., Silow, E., Sitoki, L. M., Tamatamah, R., & McIntyre, P. B. (2017).

1079   Global patterns in lake ecosystem responses to warming based on the temperature

1080   dependence of metabolism. *Global Change Biology*, *23*(5), 1881–1890.

1081   https://doi.org/10.1111/gcb.13459

1082   Ladwig, R., Hanson, P. C., Dugan, H. A., Carey, C. C., Zhang, Y., Shu, L., Duffy, C. J., &

1083   Cobourn, K. M. (2021). Lake thermal structure drives interannual variability in summer

1084   anoxia dynamics in a eutrophic lake over 37 years. *Hydrology and Earth System*

1085   *Sciences*, *25*(2), 1009–1032. https://doi.org/10.5194/hess-25-1009-2021

1086 Lathrop, R., & Carpenter, S. (2014). Water quality implications from three decades of

1087   phosphorus loads and trophic dynamics in the Yahara chain of lakes. *Inland Waters*,

1088   *4*(1), 1–14. https://doi.org/10.5268/IW-4.1.680

1089 Lei, R., Leppäranta, M., Erm, A., Jaatinen, E., & Pärn, O. (2011). Field investigations of

1090   apparent optical properties of ice cover in Finnish and Estonian lakes in winter 2009.

1091   *Estonian Journal of Earth Sciences*, *60*(1), 50. https://doi.org/10.3176/earth.2011.1.05

1092 Livingstone, D. M., & Imboden, D. M. (1996). The prediction of hypolimnetic oxygen

1093   profiles: A plea for a deductive approach. *Canadian Journal of Fisheries and Aquatic*

1094   *Sciences*, *53*(4), 924–932. https://doi.org/10.1139/f95-230

1095 Loose, B., & Schlosser, P. (2011). Sea ice and its effect on CO_2 flux between the atmosphere

1096   and the Southern Ocean interior. *Journal of Geophysical Research: Oceans*, *116*(C11),

1097   2010JC006509. https://doi.org/10.1029/2010JC006509

1098 Lovett, G. M., Cole, J. J., & Pace, M. L. (2006). Is Net Ecosystem Production Equal to

1099   Ecosystem Carbon Accumulation? *Ecosystems*, *9*(1), 152–155.

1100   https://doi.org/10.1007/s10021-005-0036-3

1101 Maerki, M., Müller, B., Dinkel, C., & Wehrli, B. (2009). Mineralization pathways in lake

1102   sediments with different oxygen and organic carbon supply. *Limnology and*

1103   *Oceanography*, *54*(2), 428–438. https://doi.org/10.4319/lo.2009.54.2.0428

1104 Magee, M. R., McIntyre, P. B., Hanson, P. C., & Wu, C. H. (2019). Drivers and Management

1105   Implications of Long-Term Cisco Oxythermal Habitat Decline in Lake Mendota, WI.

1106   *Environmental Management*, *63*(3), 396–407. https://doi.org/10.1007/s00267-018-

1107   01134-7

1108

1109

Magnuson, J., Carpenter, S., & Stanley, E. (2020). *North Temperate Lakes LTER: Chemical Limnology of Primary Study Lakes: Nutrients, pH and Carbon 1981 - current* [Data set]. Environmental Data Initiative. https://doi.org/10.6073/PASTA/8359D27BBD91028F222D923A7936077D

Magnuson, J. J., Benson, B. J., & Kratz, T. K. (2006). *Long-term dynamics of lakes in the landscape: Long-term ecological research on north temperate lakes.* Oxford University Press on Demand.

Magnuson, J. J., Carpenter, S. R., & Stanley, E. H. (2022). *North Temperate Lakes LTER: Physical Limnology of Primary Study Lakes 1981 - current* [Data set]. Environmental Data Initiative. https://doi.org/10.6073/PASTA/925D94173F35471F699B5BC343AA1128

McClure, R. P., Lofton, M. E., Chen, S., Krueger, K. M., Little, J. C., & Carey, C. C. (2020). The Magnitude and Drivers of Methane Ebullition and Diffusion Vary on a Longitudinal Gradient in a Small Freshwater Reservoir. *Journal of Geophysical Research: Biogeosciences*, *125*(3). https://doi.org/10.1029/2019JG005205

McCullough, I. M., Dugan, H. A., Farrell, K. J., Morales-Williams, A. M., Ouyang, Z., Roberts, D., Scordo, F., Bartlett, S. L., Burke, S. M., Doubek, J. P., Krivak-Tetley, F. E., Skaff, N. K., Summers, J. C., Weathers, K. C., & Hanson, P. C. (2018). Dynamic modeling of organic carbon fates in lake ecosystems. *Ecological Modelling*, *386*, 71–82. https://doi.org/10.1016/j.ecolmodel.2018.08.009

1130

1131 Mi, C., Shatwell, T., Ma, J., Wentzky, V. C., Boehrer, B., Xu, Y., & Rinke, K. (2020). The

1132   formation of a metalimnetic oxygen minimum exemplifies how ecosystem dynamics

1133   shape biogeochemical processes: A modelling study. *Water Research*, *175*, 115701.

1134   https://doi.org/10.1016/j.watres.2020.115701

1135 Morris, M. D. (1991). Factorial Sampling Plans for Preliminary Computational Experiments.

1136   *Technometrics*, *33*(2), 161–174. https://doi.org/10.1080/00401706.1991.10484804

1137 Müller, B., Bryant, L. D., Matzinger, A., & Wüest, A. (2012). Hypolimnetic Oxygen

1138   Depletion in Eutrophic Lakes. *Environmental Science & Technology*, *46*(18), 9964–

1139   9971. https://doi.org/10.1021/es301422r

1140 Nürnberg, G. K. (1995). Quantifying anoxia in lakes. *Limnology and Oceanography*, *40*(6),

1141   1100–1111. https://doi.org/10.4319/lo.1995.40.6.1100

1142 Nürnberg, G. K. (2004). Quantified Hypoxia and Anoxia in Lakes and Reservoirs. *The*

1143   *Scientific World JOURNAL*, *4*, 42–54. https://doi.org/10.1100/tsw.2004.5

1144 Odum, H. T. (1956). Primary Production in Flowing Waters. *Limnology and Oceanography*,

1145   *1*(2), 102–117. https://doi.org/10.4319/lo.1956.1.2.0102

1146 Platt, T., Gallegos, C., & Harrison, W. (1980). Photoinhibition of photosynthesis in natural

1147   assemblages of marine phytoplankton. *Journal of Marine Research*, *38*(4), 687–701.

1148 Prairie, Y. T., Bird, D. F., & Cole, J. J. (2002). The summer metabolic balance in the

1149   epilimnion of southeastern Quebec lakes. *Limnology and Oceanography*, *47*(1), 316–

1150   321. https://doi.org/10.4319/lo.2002.47.1.0316

1151 Qu, Y., & Duffy, C. J. (2007). A semidiscrete finite volume formulation for multiprocess

1152   watershed simulation: MULTIPROCESS WATERSHED SIMULATION. *Water*

1153   *Resources Research*, *43*(8). https://doi.org/10.1029/2006WR005752

1154 Rautio, M., Mariash, H., & Forsström, L. (2011). Seasonal shifts between autochthonous and

1155   allochthonous carbon contributions to zooplankton diets in a subarctic lake. *Limnology*

1156   *and Oceanography*, *56*(4), 1513–1524. https://doi.org/10.4319/lo.2011.56.4.1513

1157 Read, J. S., Hamilton, D. P., Jones, I. D., Muraoka, K., Winslow, L. A., Kroiss, R., Wu, C.

1158   H., & Gaiser, E. (2011). Derivation of lake mixing and stratification indices from high-

1159   resolution lake buoy data. *Environmental Modelling & Software*, *26*(11), 1325–1336.

1160   https://doi.org/10.1016/j.envsoft.2011.05.006

1161 Read, J. S., Zwart, J. A., Kundel, H., Corson-Dosch, H. R., Hansen, G. J. A., Vitense, K.,

1162   Appling, A. P., Oliver, S. K., & Platt, L. (2021). *Data release: Process-based*

1163   *predictions of lake water temperature in the Midwest US* [Data set]. U.S. Geological

1164   Survey. https://doi.org/10.5066/P9CA6XP8

1165 Reynolds, C. S., Oliver, R. L., & Walsby, A. E. (1987). Cyanobacterial dominance: The role

1166   of buoyancy regulation in dynamic lake environments. *New Zealand Journal of Marine*

1167   *and Freshwater Research*, *21*(3), 379–390.

1168   https://doi.org/10.1080/00288330.1987.9516234

1169 Rhodes, J., Hetzenauer, H., Frassl, M. A., Rothhaupt, K.-O., & Rinke, K. (2017). Long-term

1170   development of hypolimnetic oxygen depletion rates in the large Lake Constance.

1171   *Ambio*, *46*(5), 554–565. https://doi.org/10.1007/s13280-017-0896-8

1172   Richardson, D. C., Carey, C. C., Bruesewitz, D. A., & Weathers, K. C. (2017). Intra- and

1173   inter-annual variability in metabolism in an oligotrophic lake. *Aquatic Sciences*, *79*(2),

1174   319–333. https://doi.org/10.1007/s00027-016-0499-7

1175   Rippey, B., & McSorley, C. (2009). Oxygen depletion in lake hypolimnia. *Limnology and*

1176   *Oceanography*, *54*(3), 905–916. https://doi.org/10.4319/lo.2009.54.3.0905

1177   Schindler, D. W., Carpenter, S. R., Chapra, S. C., Hecky, R. E., & Orihel, D. M. (2016).

1178   Reducing Phosphorus to Curb Lake Eutrophication is a Success. *Environmental Science*

1179   *& Technology*, *50*(17), 8923–8929. https://doi.org/10.1021/acs.est.6b02204

1180   Snortheim, C. A., Hanson, P. C., McMahon, K. D., Read, J. S., Carey, C. C., & Dugan, H. A.

1181   (2017). Meteorological drivers of hypolimnetic anoxia in a eutrophic, north temperate

1182   lake. *Ecological Modelling*, *343*, 39–53.

1183   https://doi.org/10.1016/j.ecolmodel.2016.10.014

1184   Sobek, S., Tranvik, L. J., Prairie, Y. T., Kortelainen, P., & Cole, J. J. (2007). Patterns and

1185   regulation of dissolved organic carbon: An analysis of 7,500 widely distributed lakes.

1186   *Limnology and Oceanography*, *52*(3), 1208–1219.

1187   https://doi.org/10.4319/lo.2007.52.3.1208

1188   Soetaert, K., & Petzoldt, T. (2010). Inverse Modelling, Sensitivity and Monte Carlo Analysis

1189   in *R* Using Package **FME**. *Journal of Statistical Software*, *33*(3).

1190   https://doi.org/10.18637/jss.v033.i03

1191

1192

1193   Solomon, C. T., Bruesewitz, D. A., Richardson, D. C., Rose, K. C., Van De Bogert, M. C.,

1194   Hanson, P. C., Kratz, T. K., Larget, B., Adrian, R., Babin, B. L., Chiu, C.-Y., Hamilton,

1195   D. P., Gaiser, E. E., Hendricks, S., Istvànovics, V., Laas, A., O'Donnell, D. M., Pace, M.

1196   L., Ryder, E., … Zhu, G. (2013). Ecosystem respiration: Drivers of daily variability and

1197   background respiration in lakes around the globe. *Limnology and Oceanography*, *58*(3),

1198   849–866. https://doi.org/10.4319/lo.2013.58.3.0849

1199   Solomon, C. T., Jones, S. E., Weidel, B. C., Buffam, I., Fork, M. L., Karlsson, J., Larsen, S.,

1200   Lennon, J. T., Read, J. S., Sadro, S., & Saros, J. E. (2015). Ecosystem Consequences of

1201   Changing Inputs of Terrestrial Dissolved Organic Matter to Lakes: Current Knowledge

1202   and Future Challenges. *Ecosystems*, *18*(3), 376–389. https://doi.org/10.1007/s10021-

1203   015-9848-y

1204   Staehr, P. A., Bade, D., Van de Bogert, M. C., Koch, G. R., Williamson, C., Hanson, P.,

1205   Cole, J. J., & Kratz, T. (2010). Lake metabolism and the diel oxygen technique: State of

1206   the science: Guideline for lake metabolism studies. *Limnology and Oceanography:*

1207   *Methods*, *8*(11), 628–644. https://doi.org/10.4319/lom.2010.8.0628

1208   Steinsberger, T., Schwefel, R., Wüest, A., & Müller, B. (2020). Hypolimnetic oxygen

1209   depletion rates in deep lakes: Effects of trophic state and organic matter accumulation.

1210   *Limnology and Oceanography*, *65*(12), 3128–3138. https://doi.org/10.1002/lno.11578

1211   Thorp, J. H., & Delong, M. D. (2002). Dominance of autochthonous autotrophic carbon in

1212   food webs of heterotrophic rivers. *Oikos*, *96*(3), 543–550.

1213   https://doi.org/10.1034/j.1600-0706.2002.960315.x

Toming, K., Kotta, J., Uuemaa, E., Sobek, S., Kutser, T., & Tranvik, L. J. (2020). Predicting

    lake dissolved organic carbon at a global scale. *Scientific Reports*, *10*(1), 8471.

    https://doi.org/10.1038/s41598-020-65010-3

Tranvik, L. J. (1998). Degradation of Dissolved Organic Matter in Humic Waters by

    Bacteria. In D. O. Hessen & L. J. Tranvik (Eds.), *Aquatic Humic Substances* (Vol. 133,

    pp. 259–283). Springer Berlin Heidelberg. https://doi.org/10.1007/978-3-662-03736-

    2_11

Webster, K. E., Kratz, T. K., Bowser, C. J., Magnuson, J. J., & Rose, W. J. (1996). The

    influence of landscape position on lake chemical responses to drought in northern

    Wisconsin. *Limnology and Oceanography*, *41*(5), 977–984.

    https://doi.org/10.4319/lo.1996.41.5.0977

Wilkinson, G. M., Pace, M. L., & Cole, J. J. (2013). Terrestrial dominance of organic matter

    in north temperate lakes: ORGANIC MATTER COMPOSITION IN LAKES. *Global

    Biogeochemical Cycles*, *27*(1), 43–51. https://doi.org/10.1029/2012GB004453

Williamson, C. E., Dodds, W., Kratz, T. K., & Palmer, M. A. (2008). Lakes and streams as

    sentinels of environmental change in terrestrial and atmospheric processes. *Frontiers in

    Ecology and the Environment*, *6*(5), 247–254. https://doi.org/10.1890/070140

Winslow, L. A., Zwart, J. A., Batt, R. D., Dugan, H. A., Woolway, R. I., Corman, J. R.,

    Hanson, P. C., & Read, J. S. (2016). LakeMetabolizer: An R package for estimating lake

    metabolism from free-water oxygen using diverse statistical models. *Inland Waters*,

    6(4), 622–636. https://doi.org/10.1080/IW-6.4.883